X-Structured Precoder Designs for Spatial-Multiplexing MIMO and MIMO Relay Systems

Chun-Tao Lin, *Member, IEEE*, and Wen-Rong Wu, *Member, IEEE*

***Abstract*—In multiple-input–multiple-output (MIMO) transmission, precoding has been considered a promising technique to improve the system performance. In general, the criterion of precoder design depends on the detector used at the receiver. For the maximum-likelihood (ML) detector, the criterion is to maximize the minimum distance of the received signal constellation. Unfortunately, the derivation of the optimum solution is known to be difficult, and suboptimum solutions have then been developed. One promising approach confines the precoder having an X-structure. Several methods have been developed to solve the X-structured precoder. However, most of them use numerical searches to find their solutions and require lookup tables during run time. In this paper, we propose a systematic design method to solve the problems. The proposed precoder has a simple closed-form expression, and no numerical searches and lookup tables are required. Simulation results show that the proposed method can yield almost the same performance as the existing methods. We also consider the problem of joint source/relay precoder design in a two-hop amplify-and-forward MIMO relay system. Since the problem is much more involved and a closed-form solution is intractable to find, we then extend the use of the proposed X-structured precoder so that the problem can be reformulated as a simple scalar-valued optimization problem. Simulations show that the proposed method can significantly outperform existing joint design methods.**

***Index Terms*—Free distance, geometric mean decomposition (GMD), maximum-likelihood (ML) detection, MIMO, multiple-input–multiple-output (MIMO) relay systems, spatial multiplexing, X-structured precoder.**

I. Introduction

In RECENT years, the multiple-input–multiple-output (MIMO) technique has been widely adopted in wireless communication systems. In MIMO systems, it is well known that transmission with spatial multiplexing can provide higher spectral efficiency without bandwidth expansion [1], [2]. However, its performance heavily depends on the condition number of the channel matrix [3]. Precoding is an effective method to overcome this problem. With a low-rate feedback link, channel state information (CSI) is acquired at the transmitter, and a precoder can then be designed and applied.

The precoder design problem has been extensively studied in the literature. For the mutual information criterion, a method that is referred to as mercury/water-filling [4] was proposed for parallel Gaussian channels, and the obtained precoder, being diagonal, is shown to be the optimum power-allocation scheme. For general MIMO channels, an iterative algorithm was proposed in [5]; however, optimality is not guaranteed. The globally optimum and low-complexity suboptimum precoders have been also proposed in [6] and [7], respectively. Except for mutual information, there are also other criteria used for the precoder design. Precoders that maximize the signal-to-noise ratio (SNR) or achieve the minimum mean square error (MMSE) were developed for linear receivers in [8]–[11]. Although the computational complexity of linear receivers is low, the performance is often not satisfactory. Two nonlinear receivers are well known, i.e., successive interference cancelation (SIC) and maximum-likelihood (ML) detection. The optimum precoder for the QR-SIC receiver [12], minimizing the block error rate (BLER), has been solved with geometric mean decomposition (GMD) [13], [14]. In addition, the optimum precoder for the MMSE-SIC receiver was also solved with uniform channel decomposition [15]. It is known that the performance of an ML receiver is dominated by the minimum distance of received signal constellations, which is referred to as free distance. It is a common criterion used for the precoder design of an ML detector [16]–[20]. Unfortunately, finding the precoder that maximizes the free distance is known to be difficult; the optimum precoder remains unsolved. Note that mutual information can have a lower bound expressed by a function of free distance, and the bound will become tight when the SNR is high [7]. However, the solutions in [5]–[7] do not have closed-form expressions; their implementations require high computational complexity.

Recently, a promising suboptimum approach for the ML receiver has been developed. It first adopts singular value decomposition (SVD) to transform the MIMO channel into parallel subchannels. Then, the subchannels are paired to obtain a set of 2×2 MIMO subsystems, and 2×2 subprecoders are designed to maximize the free distance in the MIMO subsystems. We refer to this approach as precoding with X-structure, which has been considered in [17]–[19]. Precoding with X-structure not only facilitates the precoder design but yields

Manuscript received September 4, 2012; revised February 13, 2013; accepted April 28, 2013. Date of publication May 22, 2013; date of current version November 6, 2013. This work was supported in part by the National Science Council under Grant NSC-101-2221-E-009-095-MY3. This paper was presented in part at the 2012 IEEE Global Communications Conference. The review of this paper was coordinated by Dr. Y. Ma.

The authors are with the Institute of Communications Engineering, National Chiao Tung University, Hsinchu 300, Taiwan (e-mail: tow.cm91g@nctu.edu.tw; wrwu@faculty.nctu.edu.tw).

Digital Object Identifier 10.1109/TVT.2013.2264688

a low-complexity ML receiver as well since we only have to deal with 2×2 MIMO subsystems. For 4-quadrature amplitude modulation (QAM), the optimum complex-valued subprecoder was first found in [16]. The result was extended to higher QAM constellations in [20]; however, optimality no longer held. Recently, an orthogonal subprecoder derived from a rotation matrix has been proposed in [18]. The advantage of this approach is that the design complexity can be reduced. However, the closed-form expression of the optimum rotation angle is only available for 4-QAM. A numerical search is required for the angle in higher QAM constellations. More recently, an optimum real-valued subprecoder has been developed [19]. It also requires the numerical search in design and lookup tables in run time. In this paper, we propose a design method for the X-structured precoder. The main idea is using the GMD method in the subprecoder design. With the proposed method, no numerical searches are required in the design phase, and no lookup tables are required during the application phase. Simulation results show that the performance of the proposed method is almost as good as the existing methods.

In recent years, cooperative communications have been considered as a promising method to improve the performance of point-to-point MIMO systems [21], [22]. By employing relays between the source and the destination, the signal can be transmitted via the source-to-relay and then the relay-to-destination link. Multiple antennas can be equipped at each node to form a MIMO relay system. In the MIMO relay system, both the source and relay nodes can conduct precoding, which is referred to as joint source/relay precoding. Several joint precoder designs for amplify-and-forward (AF) MIMO relay systems have been proposed. In [23] and [24], the precoders maximizing the channel capacity were developed. In [25]–[31], the precoders using the MMSE criterion were designed for the linear receivers. To the best of our knowledge, the joint precoder design in the MIMO relay system with an ML receiver has yet to be considered. We then extend the proposed method to the MIMO relay system. However, the problem becomes much more involved in this case, and a closed-form solution is difficult to obtain. To solve the problem, we propose iterative methods to derive the source and relay precoders alternatingly. First, assume that the relay precoder is given; the source precoder design can then be easily solved by the proposed MIMO precoder. Then, with the solved source precoder, the relay precoder can be solved and updated. The derivation of the relay precoder for a given source precoder, however, is much more complicated due to the fact that the MIMO relay channel is a nonlinear and complicated function of the relay precoder. We then propose two methods overcoming the problem such that the relay precoder can be efficiently solved with the Karush–Kuhn–Tucker (KKT) conditions [32]. Simulation results show that the proposed methods significantly outperform existing methods.

The remainder of this paper is organized as follows: Section II briefs the system model we use. Sections III and IV describe the proposed design methods for MIMO and MIMO relay systems, respectively. Section V reports the simulation results, and finally, Section VI draws conclusions.

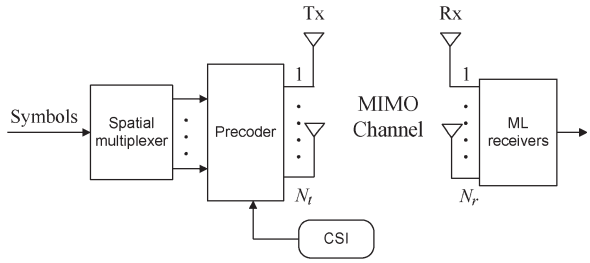

Fig. 1. System model for a precoded spatial-multiplexing MIMO system.

II. System and Signal Models

Consider a precoded spatial-multiplexing MIMO system with N_t transmit antennas and N_r receive antennas, as described in Fig. 1. Let $\mathbf{x} = [x_1, x_2, \ldots, x_M]^T$ denote the $M \times 1$ symbol vector, where $(.)^T$ represents the transpose operation. In spatial multiplexing, each entry of $\mathbf{x}$ is independently chosen from a finite-set constellation $\mathcal{X}$. For L-QAM, $\mathcal{X}$ is given by

$$\mathcal{X} = \frac{1}{\sqrt{K}} \left\{ \pm a \pm bj | a, b \in (1, 3, \ldots, \sqrt{L} - 1) \right\} \quad (1)$$

where $K = (2/3)(L-1)$. Let $\mathbf{H}$ denote the $N_r \times N_t$ channel matrix, which is assumed to be perfectly known at both the transmitter and the receiver. In addition, we assume that $M = N_t \leq N_r$ and that $\mathbf{H}$ remains unchanged for a given precoding period. Using the CSI at the transmitter, we can design an $N_t \times M$ precoding matrix $\mathbf{M}$ and conduct precoding by left-multiplying $\mathbf{M}$ on $\mathbf{x}$. In general, the power of $\mathbf{M}$ has to be constrained, i.e., $\mathrm{tr}\{\mathbf{M}^H\mathbf{M}\} = P_T$, where $(.)^H$ is the Hermitian transpose operation, and P_T is a constant. The received symbol vector can then be expressed as

$$\mathbf{y} = \mathbf{HMx} + \mathbf{n} \quad (2)$$

where $\mathbf{n}$ is the Gaussian noise vector. Assume that each entry of $\mathbf{n}$ is identically and independently distributed (i.i.d.) with the covariance matrix of $\sigma_n^2 \mathbf{I}_{N_r}$, where σ_n^2 is the noise variance, and $\mathbf{I}_{N_r}$ denotes an $N_r \times N_r$ identity matrix. At the receiver, the ML detector searches all possible symbol vectors to obtain an estimate $\hat{\mathbf{x}}$ such that

$$\hat{\mathbf{x}} = \min_{\mathbf{x} \in \mathcal{X}^M} \|\mathbf{y} - \mathbf{HMx}\| \quad (3)$$

where $\mathcal{X}^M$ is a set consisting of all possible transmitted symbol vectors. Let $d_{i,j}$ denote the distance between two distinct received symbol vectors $\mathbf{HMx}_i$ and $\mathbf{HMx}_j$. The free distance of a MIMO system is then defined as

$$d_{\mathrm{free}} \triangleq \min_{i \neq j} d_{i,j} = \min_{\mathbf{x}_i, \mathbf{x}_j \in \mathcal{X}^M, \mathbf{x}_i \neq \mathbf{x}_j} \|\mathbf{HM}(\mathbf{x}_i - \mathbf{x}_j)\|. \quad (4)$$

The error probability of (3) can then be represented as

$$P_e = \frac{1}{L^M} \sum_{i=1}^{L^M} \sum_{j=1, j \neq i}^{L^M} P_{ij} \quad (5)$$

where P_{ij} is the probability that transmitted symbol vector $\mathbf{x}_i$ is falsely detected to some other $\mathbf{x}_j$. If d_{free} is much smaller than other $d_{i,j}$'s, then we can assume that P_e will be dominated

by (4). Under this assumption, the design criterion for $\mathbf{M}$ can be chosen as maximizing the free distance of a MIMO system. This problem is known to be difficult since d_{free} depends on discrete set $\mathcal{X}^M$. Note that error probability P_e is also referred to as the BLER in this paper.

A recently developed method to overcome the problem is the application of the X-structured precoder [17]–[19]. To do that, $\mathbf{H}$ is first transformed into parallel subchannels, and precoding is applied on the subchannels. Using SVD, we can have $\mathbf{H} = \mathbf{U}\mathbf{\Sigma}\mathbf{V}^H$, where $\mathbf{U}$ is an $N_r \times M$ matrix, $\mathbf{\Sigma}$ is an $M \times M$ real-valued diagonal matrix, and $\mathbf{V}^H$ is an $M \times N_t$ matrix. Note that $\mathbf{U}^H\mathbf{U} = \mathbf{V}^H\mathbf{V} = \mathbf{I}_M$ and $\mathbf{\Sigma} = \text{diag}(\lambda_1, \lambda_2, \ldots, \lambda_M)$, where λ_i's are the singular values of $\mathbf{H}$. Let λ_i's be arranged in a descending order, i.e., $\lambda_1 \geq \lambda_2 \geq \cdots \geq \lambda_M > 0$ and $\mathbf{M} = \mathbf{V}\mathbf{F}$, where $\mathbf{F}$ is an $M \times M$ matrix. Left-multiplying $\mathbf{U}^H$ on $\mathbf{y}$, we can have the equivalent received signal model as

$$\mathbf{r} = \mathbf{\Sigma}\mathbf{F}\mathbf{x} + \mathbf{n}' \tag{6}$$

where $\mathbf{r} = \mathbf{U}^H\mathbf{y}$ and $\mathbf{n}' = \mathbf{U}^H\mathbf{n}$ is the noise vector with the same covariance matrix as $\mathbf{n}$. In what follows, we will refer to $\mathbf{F}$ as the precoder since $\mathbf{M}$ can be derived if $\mathbf{F}$ has been obtained. Note that the power constraint of the precoder still holds, i.e., $\text{tr}\{\mathbf{M}^H\mathbf{M}\} = \text{tr}\{\mathbf{F}^H\mathbf{F}\}$. Therefore, we can have the problem reformulated as

$$\begin{aligned} &\max_{\mathbf{F}} \quad \min_{\mathbf{x},\mathbf{x}' \in \mathcal{X}^M, \mathbf{x} \neq \mathbf{x}'} \|\mathbf{\Sigma}\mathbf{F}(\mathbf{x} - \mathbf{x}')\| \\ &\text{s.t.} \\ &\text{tr}\,\{\mathbf{F}^H\mathbf{F}\} = P_T. \end{aligned} \tag{7}$$

The diagonal structure of $\mathbf{\Sigma}$ in (7) greatly facilitates the derivation of the solution. The key idea is to apply an X-structure on $\mathbf{F}$, which means that subchannels ordered according to their singular values are paired to obtain a set of 2×2 subsystems, and $2\times$ 2 subprecoders are designed to maximize the free distance of the subsystems.

We first focus on the design of a $2\times$ 2 precoder in (7). For $M = 2$, $\mathbf{\Sigma}$ can be expressed as

$$\mathbf{\Sigma} = \begin{bmatrix} \lambda_1 & 0 \\ 0 & \lambda_2 \end{bmatrix} = \rho \begin{bmatrix} \cos\gamma & 0 \\ 0 & \sin\gamma \end{bmatrix} \tag{8}$$

where $\rho = \sqrt{\lambda_1^2 + \lambda_2^2}$ is the channel gain, and $\gamma = \tan^{-1}(\lambda_2/\lambda_1)$ is an angle related to the channel. Clearly, $0 < \gamma \leq (\pi/4)$ so that $\lambda_1 \geq \lambda_2$ is satisfied. With SVD, $\mathbf{F}$ can be written as $\mathbf{F} = \mathbf{U}_F\mathbf{\Sigma}_F\mathbf{V}_F^H$, where both $\mathbf{U}_F$ and $\mathbf{V}_F$ are 2×2 unitary matrices, and $\mathbf{\Sigma}_F$ is a 2×2 diagonal matrix. It has been shown in [16] that $\mathbf{U}_F$ can be an identity matrix without affecting the system performance for symmetric QAM modulations. Letting $\mathbf{V}_F^H = \mathbf{V}_{F,1}\mathbf{V}_{F,2}$ [16], we can have $\mathbf{F}$ expressed as follows:

$$\begin{aligned} \mathbf{F} &= \sqrt{P_T}\mathbf{\Sigma}_F\mathbf{V}_{F,1}\mathbf{V}_{F,2} \\ &= \sqrt{P_T} \underbrace{\begin{bmatrix} \cos\psi & 0 \\ 0 & \sin\psi \end{bmatrix}}_{\mathbf{\Sigma}_F} \underbrace{\begin{bmatrix} \cos\theta & \sin\theta \\ -\sin\theta & \cos\theta \end{bmatrix}}_{\mathbf{V}_{F,1}} \underbrace{\begin{bmatrix} 1 & 0 \\ 0 & e^{i\varphi} \end{bmatrix}}_{\mathbf{V}_{F,2}} \end{aligned} \tag{9}$$

where $0 \leq \psi \leq (\pi/2)$, $0 \leq \theta \leq (\pi/4)$, and $0 \leq \varphi \leq (\pi/2)$. Given a set of difference vectors, the subprecoder can be found with (8) and (9) by a numerical search over all possible values of ψ, θ, and φ. In [16], the optimum subprecoder for 4-QAM was found, and its application to higher QAM constellations was studied in [20]. Note that the subprecoder has complex values. To reduce the design complexity, $\mathbf{V}_{F,2}$ in (9) can be set as an identity matrix, yielding a real-valued subprecoder [19]. For further reduction of design complexity, $\mathbf{\Sigma}_F$ can be set as an identity matrix as well, giving an orthogonal subprecoder [18]. As mentioned, most existing subprecoders require numerical searches in design or lookup tables in run time. In this paper, we propose a design method to avoid these problems.

III. Proposed Subprecoders for Multiple-Input–Multiple-Output Systems

To avoid numerical search or lookup tables, we propose a systematic design giving simple closed-form expressions for any QAM sizes. To do that, we consider an alternative design criterion in (7). Instead of maximizing the free distance itself, we propose maximizing a lower bound.

A. Lower Bound for Free Distance

Considering the QR decomposition (QRD) of a full column-rank matrix $\mathbf{H}$, we can have $\mathbf{H} = \mathbf{Q}\mathbf{R}$, where $\mathbf{Q}$ is an $N_r \times N_t$ columnwise orthonormal matrix, and $\mathbf{R}$ is an $N_t \times N_t$ upper-triangular matrix with positive real-valued diagonal entries. Let $d_{\min}$ denote the minimum distance of a QAM constellation. From (1), we have $d_{\min} = 2/\sqrt{K}$. In [14], it was shown that the free distance of a spatial-multiplexing MIMO system can be lower bounded by

$$d_{\text{free}} \geq \min_i \mathbf{R}(i,i) d_{\min} = [\mathbf{R}]_{\min} \frac{2}{\sqrt{K}} \tag{10}$$

where $\mathbf{R}(i,i)$ denotes the ith diagonal entry of $\mathbf{R}$, $[\mathbf{R}]_{\min}$ represents the minimum value among $\mathbf{R}(i,i)$'s, and the equality holds when all $\mathbf{R}(i,i)$'s are equal [14]. It can be seen that the free distance is dominated by $[\mathbf{R}]_{\min}$ and K. Note that K is independent of the channel matrix. Hence, maximizing the lower bound of the free distance is equivalent to maximizing $[\mathbf{R}]_{\min}$. With a unitary precoder, the QRD of the equivalent channel will have the property that $\prod_{i=1}^{N_t} \mathbf{R}(i,i) = C$, where C is a constant. Clearly, the lower bound in (10) is maximized when $\mathbf{R}$ has equal diagonal entries. This precoder can be obtained by GMD given by [13], [14]

$$\mathbf{H} = \tilde{\mathbf{Q}}\tilde{\mathbf{R}}\mathbf{P}^H \tag{11}$$

where $\tilde{\mathbf{Q}}$ is an $N_r \times N_t$ columnwise orthonormal matrix, $\mathbf{P}$ is an $N_t \times N_t$ unitary matrix, and $\tilde{\mathbf{R}}$ is an $N_t \times N_t$ upper triangular matrix having equal diagonal entries. From (11), we can have $\mathbf{H}\mathbf{P} = \tilde{\mathbf{Q}}\tilde{\mathbf{R}}$. In other words, $\mathbf{P}$ can be used as a precoder so that the lower bound in (10) can be maximized.

It can be seen that each diagonal element of $\tilde{\mathbf{R}}$ is equal to the geometric mean of $\mathbf{R}(i,i)$'s, i.e.,

$$\tilde{\mathbf{R}}(i,i) = \left(\prod_{i=1}^{N_t} \mathbf{R}(i,i)\right)^{\frac{1}{N_t}}. \tag{12}$$

Note that $\mathbf{P}$ is independent of the QAM constellation, which is a great advantage when designing the precoder for the ML receiver. Although the GMD method is analytically tractable, its corresponding free distance will be significantly degraded for ill-conditioned channels. To overcome the problem, we propose a method described in the following.

B. GMD-Based Subprecoder With Rank Deficiency

As discussed, we now focus on a 2×2 subsystem. Note that for $\mathbf{\Sigma}$ with $M = 2$, $\mathbf{F}_{\mathrm{GMD}}$ has a simple expression as

$$\mathbf{F}_{\mathrm{GMD}} = \sqrt{\frac{P_T}{2}} \begin{bmatrix} \sqrt{\frac{\lambda_2}{\lambda_1+\lambda_2}} & -\sqrt{\frac{\lambda_1}{\lambda_1+\lambda_2}} \\ \sqrt{\frac{\lambda_1}{\lambda_1+\lambda_2}} & \sqrt{\frac{\lambda_2}{\lambda_1+\lambda_2}} \end{bmatrix}. \tag{13}$$

Furthermore, the resultant free distance can be also easily obtained by

$$d_{\mathrm{free},\mathbf{F}_{\mathrm{GMD}}} = \sqrt{P_T \rho^2 \frac{4}{K} \frac{\cos\gamma \sin\gamma}{2}}. \tag{14}$$

The derivations of (13) and (14) can be found in [14]. From (14), we can see that $d_{\mathrm{free},\mathbf{F}_{\mathrm{GMD}}} \approx 0$ as γ approaches zero. Note that γ is associated with the condition number of the channel matrix. In other words, the performance of $\mathbf{F}_{\mathrm{GMD}}$ can be significantly degraded for ill-conditioned channels. This is because $\mathbf{F}_{\mathrm{GMD}}$ is a full-rank matrix and always uses two subchannels for signal transmission. This structure constraint becomes inefficient when the value of γ is small, and too much power is allocated in the worse subchannel. This problem can be avoided by pouring all the transmit power on the stronger subchannel λ_1 and maps the two bit streams into a scalar symbol for transmission. In such case, the resultant subprecoder will be rank deficient. From (9), it is simple to see that a complex-valued rank-deficient subprecoder, which is denoted by $\mathbf{F}_{d,c}$, can be expressed as

$$\mathbf{F}_{d,c} = \sqrt{P_T} \begin{bmatrix} \cos\theta_{d,c} & \sin\theta_{d,c} e^{j\varphi_{d,c}} \\ 0 & 0 \end{bmatrix} \tag{15}$$

where $0 \le \theta_{d,c} \le (\pi/4)$, and $0 \le \varphi_{d,c} \le (\pi/2)$. With (13) and (15), we then propose a subprecoder expressed as

$$\mathbf{F}_{p,1} = \begin{cases} \underbrace{\sqrt{P_T} \begin{bmatrix} \cos\theta_{d,c} & \sin\theta_{d,c} e^{j\varphi_{d,c}} \\ 0 & 0 \end{bmatrix}}_{\mathbf{F}_{d,c}}, & \text{for } \gamma \le \gamma_1 \\ \mathbf{F}_{\mathrm{GMD}}, & \text{for } \gamma > \gamma_1. \end{cases} \tag{16}$$

By letting $N = 2^{(1/2)\log_2^L} - 1$, the optimum angles for $\mathbf{F}_{d,c}$ can be expressed as $\varphi_{d,c} = \tan^{-1}(1/(2N+\sqrt{3}))$ and $\theta_{d,c} = \tan^{-1}(2\sin\varphi_{d,c})$ [16]. Threshold γ_1 in (16) can be derived by the channel angle satisfying $d_{\mathrm{free},\mathbf{F}_{\mathrm{GMD}}} = d_{\mathrm{free},\mathbf{F}_{d,c}}$, where $d_{\mathrm{free},\mathbf{F}_{d,c}}$ denotes the corresponding free distance of $\mathbf{F}_{d,c}$. Therefore, we can have $\gamma_1 = \tan^{-1}(2/(N^2+\sqrt{3}N+2))$.

We can also use a real-valued rank-deficient subprecoder, which is denoted by $\mathbf{F}_{d,r}$, to derive another subprecoder. Note that $\mathbf{F}_{d,r}$ can be simply obtained by removing $\mathbf{V}_{F,2}$ in (9). Let $l = (1/2)\log_2(L)$ and $\theta_{d,r} = \tan^{-1}(2^{-l})$, where $l \in \{1,2,\ldots,5\}$. We then propose an alternative subprecoder as

$$\mathbf{F}_{p,2} = \begin{cases} \underbrace{\sqrt{P_T} \begin{bmatrix} \cos\theta_{d,r} & \sin\theta_{d,r} \\ 0 & 0 \end{bmatrix}}_{\mathbf{F}_{d,r}}, & \text{for } \gamma \le \gamma_2 \\ \mathbf{F}_{\mathrm{GMD}}, & \text{for } \gamma > \gamma_2. \end{cases} \tag{17}$$

With the similar method used for $\mathbf{F}_{p,1}$, we can have $\gamma_2 = \tan^{-1}(2\sin^2(\tan^{-1}(2^{-l})))$. From (16) and (17), we can see that both $\mathbf{F}_{p,1}$ and $\mathbf{F}_{p,2}$ have closed-form expressions. Thus, no lookup tables are required.

Note that the lower bound in (10) instead of d_{free} is used in our design. Optimality then becomes a main concern. Since a theoretical analysis is very difficult, we only provide a simple qualitative analysis to this problem. It is easy to see that the tightness of the lower bound in (10) is proportional to channel angle γ. For well-conditioned channels, γ is large, and the error due to the use of the lower bound will be small. For ill-conditioned channels, γ is small, and the bound will be loose; however, a rank-deficient subprecoder is used instead. The subprecoder in [18], which is assumed to be orthogonal, also suffers from performance loss for ill-conditioned channels, whereas the subprecoder in [18], which is assumed to be real, does not suffer from performance loss. When γ is small, the scheme in [19] also applies a rank-deficient subprecoder. Simulation results in Section V show that our proposed methods can provide near-optimum results.

C. Extension to MIMO Systems for $M > 2$

For a MIMO system with $M > 2$, the X-structured precoder allows a simple solution for the ML receiver. Assuming that M is even, then every two subchannels can be paired to yield $(M/2)$ subsystems. Therefore, the 2×2 subprecoders discussed in the previous sections can be directly applied. Let the subchannels be ordered with respect to their singular values. Then, the X-structured precoder pairs the ith and the $(M-i+1)$th subchannels, and the corresponding channel gain and channel angle can be expressed as $\rho_i = \sqrt{\lambda_i^2 + \lambda_{M-i+1}^2}$ and $\gamma_i = \tan^{-1}(\lambda_{M-i+1}/\lambda_i)$, respectively. Using γ_i, we can construct the resultant subprecoder $\mathbf{F}_{p,(i)}$ for the ith subsystem. Let each subprecoder have the unit-power constraint, i.e., $\mathrm{tr}\{\mathbf{F}_{p,(i)}^H \mathbf{F}_{p,(i)}\} = 1$. In addition, let $d_{\mathrm{free},i}$ denote the free distance provided by the ith subsystem, and $d_{\mathrm{free,min}}$ is the minimum value among all $d_{\mathrm{free},i}$'s. Clearly, the overall system performance is dominated by the subsystem with $d_{\mathrm{free,min}}$. Hence, we can adopt a power-allocation scheme aiming to maximize $d_{\mathrm{free,min}}$ so that the performance can be further enhanced. Let $\mathbf{\Upsilon} = \mathrm{diag}(\Upsilon_1, \Upsilon_2, \ldots, \Upsilon_{M'-1}, \Upsilon_{M'}, \Upsilon_{M'}, \Upsilon_{M'-1}, \ldots, \Upsilon_2, \Upsilon_1)$, where Υ_i is the power allocated on the ith subsystem, and M' is the number

TABLE I
COMPLEXITY COMPARISONS FOR SUBPRECODER DESIGNS

X-Structured Precoding				Decoding	
Subprecoder	SVD of $\mathbf{H}$	$\mathbf{M}$	Look-up Tables	$\mathbf{r}$	ML Detection
$\mathbf{F}_c$ [17]	$\mathcal{O}\left(N_r^2N_t+N_t^2N_r\right)$	$\mathcal{O}\left(N_tM\right)$	$\times$	$\mathcal{O}\left(N_r^2\right)$	$\mathcal{O}\left(M'L\sqrt{L}\right)$
$\mathbf{F}_r$ [19]	$\mathcal{O}\left(N_r^2N_t+N_t^2N_r\right)$	$\mathcal{O}\left(N_tM\right)$	required for $L>4$	$\mathcal{O}\left(N_r^2\right)$	$\mathcal{O}\left(M'\sqrt{L}\right)$
$\mathbf{F}_o$ [18]	$\mathcal{O}\left(N_r^2N_t+N_t^2N_r\right)$	$\mathcal{O}\left(N_tM\right)$	required for $L>4$	$\mathcal{O}\left(N_r^2\right)$	$\mathcal{O}\left(M'\sqrt{L}\right)$
Proposed $\mathbf{F}_{p,1}$	$\mathcal{O}\left(N_r^2N_t+N_t^2N_r\right)$	$\mathcal{O}\left(N_tM\right)$	$\times$	$\mathcal{O}\left(N_r^2\right)$	$\mathcal{O}\left(M'L\sqrt{L}\right)$ for smaller value of L
					$\approx\mathcal{O}\left(M'\sqrt{L}\right)$ for larger value of L
Proposed $\mathbf{F}_{p,2}$	$\mathcal{O}\left(N_r^2N_t+N_t^2N_r\right)$	$\mathcal{O}\left(N_tM\right)$	$\times$	$\mathcal{O}\left(N_r^2\right)$	$\mathcal{O}\left(M'\sqrt{L}\right)$

of subsystems. Similar to the method used in [17], the solution of Υ_i is given by

$$\Upsilon_i=\sqrt{P_T}\left(d_{\mathrm{free},i}^2\sum_{k=1}^{M'}\frac{1}{d_{\mathrm{free},k}^2}\right)^{-\frac{1}{2}}. \tag{18}$$

With (18), we can see that $\mathbf{\Upsilon}$ is to equalize the free distance among all subsystems. That means the subsystem with a smaller free distance will be allocated higher transmit power. It can be easily verified that $\Upsilon_i d_{\mathrm{free},i}\geq d_{\mathrm{free,min}}$, and hence, the performance is improved. With $\mathbf{\Upsilon}$, the resultant precoder is still of X-structure. If M is odd, the $((M+1)/2)$th symbol is then independently precoded and detected without coupling another symbol. Note that computing Υ_i requires information on $d_{\mathrm{free},i}$. In this regard, the proposed subprecoders are more efficient since the free distance can be easily calculated.

D. Complexity Comparisons

First, we use the number of floating operations (FLOPS) required in a precoding scheme as the measure for computational complexity. The complexity for conducting the SVD of $\mathbf{H}$ is $\mathcal{O}(N_r^2N_t+N_t^2N_r)$, that for calculating $\mathbf{M}$ is $\mathcal{O}(N_tM)$ FLOPS, and that for calculating $\mathbf{r}$ is $\mathcal{O}(N_r^2)$ FLOPS. The given operations are involved in all the methods. Note that both the orthogonal and real-valued precoders need lookup tables in their applications, and this is an additional overhead that is not required for the proposed precoders.

Next, we compare the ML-detection complexity in each method. It has been shown in [19] that the ML-detection complexity in a subsystem with the complex-valued precoder is a function of $\mathcal{O}(L\sqrt{L})$. The detection complexity can be reduced to $\mathcal{O}(\sqrt{L})$ when the precoder consists of real values. Thus, the ML-detection complexity associated with $\mathbf{F}_{p,1}$ is higher than that with $\mathbf{F}_{p,2}$. Nevertheless, the probability for the event that $\gamma\leq\gamma_1$ decreases for large values of L. Therefore, the detection complexity corresponding to $\mathbf{F}_{p,1}$ can be also $\mathcal{O}(\sqrt{L})$ for higher QAM constellations. The complexity comparison for all precoders is summarized in Table I.

IV. PRECODER DESIGN FOR MULTIPLE-INPUT–MULTIPLE-OUTPUT RELAY SYSTEMS

Here, we will consider the precoder design in two-hop AF MIMO relay systems. Similar to the conventional MIMO system, we can conduct precoding at both the source and relay nodes. These two precoders can be jointly optimized for further performance enhancement. Note that the ML receiver is used at the destination.

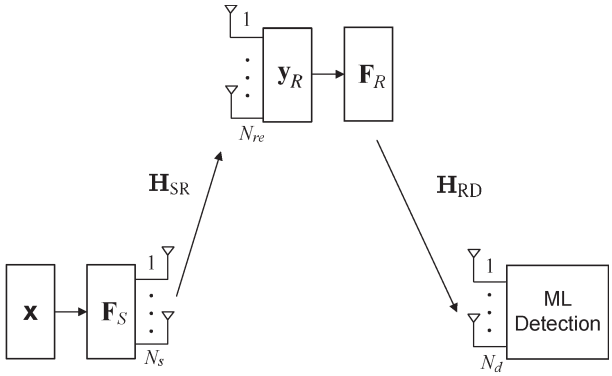

Fig. 2. System model for a precoded spatial-multiplexing MIMO relay system.

A. Problem Formulation and Source Precoder Design

The system model we consider is shown in Fig. 2. Let $\mathbf{H}_{SR}$ denote the $N_{re}\times N_s$ source-to-relay channel matrix and $\mathbf{H}_{RD}$ denote the $N_d\times N_{re}$ relay-to-destination channel matrix. In the AF MIMO relay scheme, the signal transmission is divided into two phases. In Phase I, $\mathbf{x}$ is transmitted from the source and then received at the relay. We assume that the destination cannot receive the signal from the source in Phase I due to long distance. In the scenario, the relay node can serve as a repeater for the extension of transmission coverage. Let $\mathbf{F}_S$ denote the $N_s\times M$ source precoding matrix. The received signal at the relay can then be expressed as $\mathbf{y}_R=\mathbf{H}_{SR}\mathbf{F}_S\,\mathbf{x}+\mathbf{n}_R$, where $\mathbf{n}_R$ is the Gaussian noise vector with a covariance matrix of $\sigma_{n,r}^2\mathbf{I}_{N_{re}}$. In Phase II, $\mathbf{y}_R$ is first left-multiplied by an $N_{re}\times N_{re}$ relay precoding matrix $\mathbf{F}_R$ and then retransmitted to the destination through $\mathbf{H}_{RD}$. The received signal at the destination can be expressed as

$$\mathbf{y}_D=\mathbf{H}_{RD}\mathbf{F}_R\mathbf{H}_{SR}\mathbf{F}_S\,\mathbf{x}\,+\mathbf{H}_{RD}\mathbf{F}_R\mathbf{n}_R+\mathbf{n}_D \tag{19}$$

where $\mathbf{n}_D$ is a Gaussian noise vector with a covariance matrix of $\sigma_{n,d}^2\mathbf{I}_{N_d}$. The received signal can then be rewritten as $\mathbf{y}_D=\mathbf{H}\mathbf{F}_S\mathbf{x}+\mathbf{n}$, where $\mathbf{H}=\mathbf{H}_{RD}\mathbf{F}_R\mathbf{H}_{SR}$, and $\mathbf{n}=\mathbf{H}_{RD}\mathbf{F}_R\mathbf{n}_R+\mathbf{n}_D$. It is simple to see that $\mathbf{n}$ is not white, and the covariance matrix of $\mathbf{n}$ can be found as

$$\mathbf{R}_n=\mathbb{E}[\mathbf{n}\mathbf{n}^H]=\sigma_{n,r}^2\mathbf{H}_{RD}\mathbf{F}_R\mathbf{F}_R^H\mathbf{H}_{RD}^H+\sigma_{n,d}^2\mathbf{I}_{N_d} \tag{20}$$

where $\mathbb{E}[.]$ denotes the expectation operation. To facilitate our derivation, we first conduct whitening processing on $\mathbf{y}_D$. Let $\mathbf{W}$ denote the whitening matrix. From (20), we can have

$$\mathbf{W} = \mathbf{R}_n^{-\frac{1}{2}} = \left(\sigma_{n,r}^2 \mathbf{H}_{RD}\mathbf{F}_R\mathbf{F}_R^H\mathbf{H}_{RD}^H + \sigma_{n,d}^2\mathbf{I}_{N_d}\right)^{-\frac{1}{2}}. \quad (21)$$

After whitening, the received signal can be written as

$$\tilde{\mathbf{y}}_D = \mathbf{W}\mathbf{y}_D = \tilde{\mathbf{H}}\mathbf{F}_S\mathbf{x} + \tilde{\mathbf{n}} \quad (22)$$

where $\tilde{\mathbf{n}} = \mathbf{W}\mathbf{n}$ and $\tilde{\mathbf{H}} = \mathbf{W}\mathbf{H}$ is the $N_d \times N_s$ equivalent channel matrix, which can be expanded as

$$\tilde{\mathbf{H}} = \left(\sigma_{n,r}^2 \mathbf{H}_{RD}\mathbf{F}_R\mathbf{F}_R^H\mathbf{H}_{RD}^H + \sigma_{n,d}^2\mathbf{I}_{N_d}\right)^{-\frac{1}{2}} \mathbf{H}_{RD}\mathbf{F}_R\mathbf{H}_{SR}. \quad (23)$$

The free distance corresponding to $\tilde{\mathbf{H}}$ can then be defined as

$$d_{\text{free}} = \min_{\mathbf{x}_i\mathbf{x}_j \in \mathcal{X}^M, \mathbf{x}_i \neq \mathbf{x}_j} \left\| \tilde{\mathbf{H}}\mathbf{F}_S(\mathbf{x}_i - \mathbf{x}_j) \right\|. \quad (24)$$

Therefore, the objective now is to find the precoders, i.e., $\mathbf{F}_S$ and $\mathbf{F}_R$ so that the free distance can be maximized. The optimization problem can be formulated as

$$\begin{aligned} &\max_{\mathbf{F}_S, \mathbf{F}_R} d_{\text{free}} \\ &\text{s.t.} \\ &\mathrm{C}_1 : \operatorname{tr}\left\{\mathbf{F}_S\mathbf{F}_S^H\right\} = P_{S,T} \\ &\mathrm{C}_2 : \operatorname{tr}\left\{\mathbf{F}_R\mathbf{y}_R\mathbf{y}_R^H\mathbf{F}_R^H\right\} \\ &\qquad = \operatorname{tr}\left\{\mathbf{F}_R\left(\sigma_{n,r}^2\mathbf{I}_{N_{re}} + \mathbf{H}_{SR}\mathbf{F}_S\mathbf{F}_S^H\mathbf{H}_{SR}^H\right)\mathbf{F}_R^H\right\} = P_{R,T} \end{aligned} \quad (25)$$

where C_1 and C_2 represent the transmit power constraints at the source and the relay, respectively. As we can see, solving the problem in (25) is complicated since d_{free} is a nonlinear and complicated function of $\mathbf{F}_S$ and $\mathbf{F}_R$. In addition, both precoders are coupled in constraint C_2. As a result, the optimum solution is difficult to find. To solve the problem, we propose an iterative method solving $\mathbf{F}_S$ and $\mathbf{F}_R$ alternatingly. First, we let $\mathbf{F}_R$ be given and then have the optimization as

$$\begin{aligned} &\max_{\mathbf{F}_S} \quad \min_{\mathbf{x}_i\mathbf{x}_j \in \mathcal{X}^M, \mathbf{x}_i \neq \mathbf{x}_j} \left\| \tilde{\mathbf{H}}\mathbf{F}_S(\mathbf{x}_i - \mathbf{x}_j) \right\| \\ &\text{s.t.} \\ &\operatorname{tr}\left\{\mathbf{F}_S\mathbf{F}_S^H\right\} = P_{S,T}. \end{aligned} \quad (26)$$

It is easy to see that (26) is similar to a MIMO precoder design problem. Consider the following SVDs:

$$\mathbf{H}_{RD} = \mathbf{U}_{RD}\mathbf{\Sigma}_{RD}\mathbf{V}_{RD}^H \quad \text{and} \quad \mathbf{H}_{SR} = \mathbf{U}_{SR}\mathbf{\Sigma}_{SR}\mathbf{V}_{SR}^H \quad (27)$$

where $\mathbf{U}_{RD}$, $\mathbf{V}_{RD}^H$, $\mathbf{U}_{SR}$, and $\mathbf{V}_{SR}^H$ are columnwise orthonormal matrices, both $\mathbf{\Sigma}_{SR}$ and $\mathbf{\Sigma}_{RD}$ are $M \times M$ diagonal matrices, and $\mathbf{U}_{RD}^H\mathbf{U}_{RD} = \mathbf{U}_{SR}^H\mathbf{U}_{SR} = \mathbf{V}_{RD}^H\mathbf{V}_{RD} = \mathbf{V}_{SR}^H\mathbf{V}_{SR} = \mathbf{I}_M$. Assume that $M = N_s = N_{re} \leq N_d$. We can let $\mathbf{F}_S$ be of the form

$$\mathbf{F}_S = \mathbf{V}_{SR}\mathbf{F}_S' \quad (28)$$

where $\mathbf{F}_S'$ is an $M \times M$ matrix. With (28), we can further rewrite received signal $\tilde{\mathbf{y}}_D$ as

$$\tilde{\mathbf{y}}_D = \tilde{\mathbf{H}}\mathbf{V}_{SR}\mathbf{F}_S'\mathbf{x} + \tilde{\mathbf{n}} = \tilde{\mathbf{H}}'\mathbf{F}_S'\mathbf{x} + \tilde{\mathbf{n}} \quad (29)$$

where $\tilde{\mathbf{H}}' = \tilde{\mathbf{H}}\mathbf{V}_{SR}$, which can be expanded as

$$\tilde{\mathbf{H}}' = \left(\sigma_{n,r}^2 \mathbf{H}_{RD}\mathbf{F}_R\mathbf{F}_R^H\mathbf{H}_{RD}^H + \sigma_{n,d}^2\mathbf{I}_{N_d}\right)^{-\frac{1}{2}} \times \mathbf{H}_{RD}\mathbf{F}_R\mathbf{U}_{SR}\mathbf{\Sigma}_{SR}. \quad (30)$$

Let $\tilde{\mathbf{\Sigma}}'$ denote the matrix with the singular values of $\tilde{\mathbf{H}}'$. With $\tilde{\mathbf{\Sigma}}'$, we can solve $\mathbf{F}_S'$ by applying the methods proposed in Section III. For a given $\mathbf{F}_S$, however, finding the solution of $\mathbf{F}_R$ is much more involved. This problem is investigated in the following section.

B. Relay Precoder Design

From (30), we first observe that $\tilde{\mathbf{H}}'$ is still a nonlinear and complicated function of $\mathbf{F}_R$, and finding the optimum $\mathbf{F}_R$ is still difficult. Even if the optimum solution can be found, we have to conduct a new SVD and matrix inversion when solving $\mathbf{F}_S$ at each iteration. This will greatly increase the computational complexity of the problem. To overcome these problems, we propose imposing a special structure on $\mathbf{F}_R$ such that the X-structure of $\mathbf{F}_S$ can be maintained, and at the same time, $\mathbf{F}_R$ can be solved with a closed-form solution. The main idea is to let $\mathbf{F}_R$ diagonalize the equivalent channel $\tilde{\mathbf{H}}'$. This can be easily accomplished by choosing $\mathbf{F}_R$ as

$$\mathbf{F}_R = \mathbf{V}_{RD}\mathbf{\Sigma}_R\mathbf{U}_{SR}^H \quad (31)$$

where $\mathbf{\Sigma}_R$ is an $M \times M$ diagonal matrix, which needs to be designed. With (31), we can rewrite whitening matrix $\mathbf{W}$ as follows:

$$\mathbf{W} = \left(\sigma_{n,r}^2 \mathbf{\Sigma}_{RD}\mathbf{\Sigma}_R\mathbf{\Sigma}_R^H\mathbf{\Sigma}_{RD}^H + \sigma_{n,d}^2\mathbf{I}_M\right)^{-\frac{1}{2}} \mathbf{U}_{RD}^H. \quad (32)$$

With (31) and (32), the resultant $\tilde{\mathbf{H}}'$ is an $M \times M$ diagonal matrix expressed as

$$\tilde{\mathbf{H}}' = \left(\sigma_{n,r}^2 \mathbf{\Sigma}_{RD}\mathbf{\Sigma}_R\mathbf{\Sigma}_R^H\mathbf{\Sigma}_{RD}^H + \sigma_{n,d}^2\mathbf{I}_M\right)^{-\frac{1}{2}} \mathbf{\Sigma}_{RD}\mathbf{\Sigma}_R\mathbf{\Sigma}_{SR}. \quad (33)$$

Thus, $\tilde{\mathbf{H}}'$ in (33) is diagonal and can be directly used for constructing $\mathbf{F}_S'$ without extra SVD and matrix inversion operations. In addition, the relay precoder to be determined is reduced to diagonal matrix $\mathbf{\Sigma}_R$. This can significantly reduce the complexity of the joint design.

Let $P_{e,i}$ denote the BLER of the ith subsystem. We can have the overall BLER, i.e., P_e, expressed as

$$P_e = 1 - \prod_{i=1}^{M'}(1 - P_{e,i}) \approx \sum_{i=1}^{M'} P_{e,i} \quad (34)$$

where M' is the number of the subsystems. The approximation error in (34) is neglectable under high-SNR scenarios. As discussed, $P_{e,i}$ is dominated by the free distance of the ith subsystem. Due to the whitening matrix in (32), the covariance

matrix of $\tilde{\mathbf{n}}$ is an identity matrix. Using the Chernoff bound, we can further have

$$P_e \approx \frac{1}{2}\underbrace{\sum_{i=1}^{M'} \exp^{-\frac{d_{\text{free},i}^2}{4}}}_{P_w} = \frac{1}{2}P_w. \tag{35}$$

As seen, minimizing P_w is approximately equivalent to minimizing P_e. Since directly minimizing P_w is still difficult, we then seek a lower bound from which our optimization can be conducted.

Proposition 1: Given a full-rank $\mathbf{F}'_S$, the relay precoder in (31), and the channel matrix in (33), maximizing $\det(\tilde{\mathbf{H}}'^H\tilde{\mathbf{H}}')$ is equivalent to minimizing a lower bound of P_w. The lower bound is equal to

$$M' \exp^{-\frac{1}{4}\left(\prod_{i=1}^{M'} d_{\text{free},i}^2\right)^{\frac{1}{M'}}}$$

where M' is the number of the subsystems.

Proof: To prove the proposition, we need the following lemmas. ■

Lemma 1: Let w_1 and w_2 be two positive values satisfying $w_1 + w_2 = 1$ and consider two positive values x and y. If $y \geq x \geq 1$, then the following inequality holds:

$$\exp^{-x^{w_1}y^{w_2}} \leq w_1 \exp^{-x} + w_2 \exp^{-y}. \tag{36}$$

The proof of the lemma is provided in Appendix A. With the lemma, we can then derive another lemma.

Lemma 2: Assume that $\mathbf{F}_S$, $\mathbf{\Sigma}_{SR}$, and $\mathbf{\Sigma}_{RD}$ are given. Then, P_w is lower bounded as

$$P_w \geq M' \exp^{-\frac{1}{4}\left(\prod_{i=1}^{M'} d_{\text{free},i}^2\right)^{\frac{1}{M'}}}. \tag{37}$$

The proof of the lemma is provided in Appendix B. To proceed, without loss of generality, we can first consider the system with a full-rank $\mathbf{F}'_S$. Using (14), $d_{\text{free},i}^2$ can be expressed as $d_{\text{free},i}^2 = \tilde{\mathbf{H}}'(i,i)\tilde{\mathbf{H}}'(M-i+1, M-i+1)\epsilon$ for $i = 1, 2, \ldots, M'$. Here, ϵ is a constant for a given QAM constellation and $P_{S,T}$. Then, we have

$$\prod_{i=1}^{M'} d_{\text{free},i}^2 = \epsilon^{M'}\sqrt{\det(\tilde{\mathbf{H}}'^H\tilde{\mathbf{H}}')}. \tag{38}$$

We then come to the conclusion that maximizing $\det(\tilde{\mathbf{H}}'^H\tilde{\mathbf{H}}')$ is equivalent to minimizing the lower bound in (37).

Note that the equality in (37) holds when $d_{\text{free},i}^2$'s are equal for all $i = 1, 2, \ldots, M'$. In other words, the tightness of (37) depends on the spread of $d_{\text{free},i}^2$'s. The smaller the spread is, the tighter the lower bound will be. A large spread of $d_{\text{free},i}^2$'s often means a poor channel condition, and a rank-deficient subprocoder will be used instead. In X-structured $\mathbf{F}'_S$, the ith and the $(M-i+1)$th subchannels are paired together. Therefore, all $d_{\text{free},i}^2$'s will be close. This property further tightens the lower bound in (37). From the given discussions, we see that the lower bound we use will be tight, and the errors due to the approximations applied will be small. Simulation results in Section V conform to the conjecture, and our methods can significantly improve precoding performance.

Using the fact that the arithmetic mean is greater than or equal to the geometric mean, we can easily derive another lower bound for P_w as

$$P_w \geq M' \exp^{-\frac{1}{4}\left(\sum_{i=1}^{M'} d_{\text{free},i}^2\right)^{\frac{1}{M'}}}. \tag{39}$$

The following property compares the lower bound in (37) and that in (39).

Property 1: The lower bound in (37) is tighter than that in (39).

Proof: See Appendix C. ■

Note that the result in Proposition 1 is only valid for the proposed subprecoders with which the properties of the GMD solution can be applied. For other subprecoders, (37) may not hold, and finding a solution for the precoders will become much more complicated. For Lemma 1 to apply, both x and y have to be greater than one. This translates into the fact that the BLER of the subsystem (in Lemma) must be less than 10^{-1}, which is usually satisfied in real-world applications. It is worth noting that $(\prod_{i=1}^{M'} d_{\text{free},i}^2)^{(1/M')}$ in (37) can be seen as a geometric free distance of the MIMO relay system, and it can be used to evaluate P_w. It is interesting to note that this is similar to the geometric SNR in multicarrier systems [33]. However, the geometric SNR is derived from the maximization of the channel capacity. Instead, the geometric free distance we derived here is to minimize the BLER. To proceed, let r denote the rank of $\mathbf{F}'_S$. We first solve $\mathbf{\Sigma}_R$ by assuming $r = M$. From (33), we have

$$\tilde{\mathbf{H}}'^H\tilde{\mathbf{H}}' = \mathbf{\Sigma}_{SR}^H\mathbf{\Sigma}_R^H\mathbf{\Sigma}_{RD}^H\left(\sigma_{n,r}^2\mathbf{\Sigma}_{RD}\mathbf{\Sigma}_R\mathbf{\Sigma}_R^H\mathbf{\Sigma}_{RD}^H + \sigma_{n,d}^2\mathbf{I}_M\right)^{-1} \times \mathbf{\Sigma}_{RD}\mathbf{\Sigma}_R\mathbf{\Sigma}_{SR}. \tag{40}$$

Defining $\mathbf{A} = \mathbf{\Sigma}_{RD}\mathbf{\Sigma}_R\mathbf{\Sigma}_R^H\mathbf{\Sigma}_{RD}^H$, we can have $\det(\tilde{\mathbf{H}}'^H\tilde{\mathbf{H}}')$ as

$$\det(\tilde{\mathbf{H}}'^H\tilde{\mathbf{H}}') = \det\left(\mathbf{\Sigma}_{SR}\mathbf{\Sigma}_{SR}^H\right)\det\left(\mathbf{A}\left(\sigma_{n,r}^2\mathbf{A} + \sigma_{n,d}^2\mathbf{I}_M\right)^{-1}\right). \tag{41}$$

Since $\det(\mathbf{\Sigma}_{SR}\mathbf{\Sigma}_{SR}^H)$ in (41) is independent of the relay precoder, $\mathbf{\Sigma}_R$ can then be solved through the following optimization:

$$\max_{\mathbf{\Sigma}_R} \det\left(\mathbf{A}\left(\sigma_{n,r}^2\mathbf{A} + \sigma_{n,d}^2\mathbf{I}_M\right)^{-1}\right)$$

s.t.

$$\operatorname{tr}\left\{\sigma_{n,r}^2\mathbf{\Sigma}_R\mathbf{\Sigma}_R^H + \mathbf{\Sigma}_R\mathbf{\Sigma}_{SR}\mathbf{F}'_S\mathbf{F}'^H_S\mathbf{\Sigma}_{SR}^H\mathbf{\Sigma}_R^H\right\} = P_{R,T}. \tag{42}$$

Let $\mathbf{B} = \mathbf{F}'_S\mathbf{F}'^H_S$. In addition, let $\sigma_{R,i}$, $\sigma_{sr,i}$, and $\sigma_{rd,i}$ be the ith diagonal entry of $\mathbf{\Sigma}_R$, $\mathbf{\Sigma}_{SR}$, and $\mathbf{\Sigma}_{RD}$, respectively. Taking ln operation, we can reformulate (42) as

$$\min_{\sigma_{R,i}^2} -\sum_{i=1}^{M} \ln\left(\frac{\sigma_{R,i}^2\sigma_{rd,i}^2}{\sigma_{R,i}^2\sigma_{rd,i}^2\sigma_{n,r}^2 + \sigma_{n,d}^2}\right)$$

s.t.

$$\sum_{i=1}^{M} \sigma_{R,i}^2\left(\sigma_{n,r}^2 + \mathbf{B}(i,i)\sigma_{sr,i}^2\right) = P_{R,T}. \tag{43}$$

We can see that the relay precoder design problem has been transformed into a scalar-valued optimization problem. The reformulated problem in (43) can be solved by using the KKT conditions [32]. The solution is then expressed in closed-form as

$$\sigma_{R,i}^2 = \sqrt{\frac{\mu\sigma_{n,d}^2}{\sigma_{rd,i}^2\sigma_{n,r}^2\left(\sigma_{n,r}^2+\mathbf{B}(i,i)\sigma_{sr,i}^2\right)}+\left(\frac{\sigma_{n,d}^2}{2\sigma_{rd,i}^2\sigma_{n,r}^2}\right)^2}-\frac{\sigma_{n,d}^2}{2\sigma_{rd,i}^2\sigma_{n,r}^2} \quad (44)$$

where μ is chosen to satisfy the relay power constraint. As we can see, the proposed subprecoder does lead to a simple expression of $\mathbf{\Sigma}_R$.

As seen from (44), we have to know $\mathbf{B}$ when solving the relay precoder. To simplify the problem, first, we do not consider source power allocation $\mathbf{\Upsilon}$. Thus, $\mathbf{B}$ can be expressed as

$$\mathbf{B}(i,i) = \frac{P_{S,T}}{M} \quad (45)$$

for $i = 1, 2, \ldots, M$. Using the resultant $\mathbf{\Sigma}_R$ and $\tilde{\mathbf{H}}'$, the next step is to construct $\mathbf{F}'_S$ with the methods proposed in Section III. If the channel angles of all subsystems are larger than the angle threshold, r is still equal to M. From the structure of $\mathbf{B}$ in (45), we can see that its diagonal entries are unchanged. In other words, $\mathbf{\Sigma}_R$ will not be changed by the updated $\mathbf{F}'_S$. Then, the iteration stops in just one iteration. On the other hand, if at least one subprecoder is of rank deficiency, (45) does not hold. Then, the iteration cannot stop in just one iteration. Note that the order of the diagonal entries of $\tilde{\mathbf{H}}'$ can be changed during the iteration. In such case, we have to reformulate $\mathbf{B}$ and resolve $\sigma_{R,i}^2$, which may be complicated. The following proposition states that these operations can be simplified.

Proposition 2: With the relay precoder given in (44), the diagonal entries of resultant $\tilde{\mathbf{H}}'$ exhibit a descending order when the SNR of the relay-to-destination path is much higher than that of the source-to-relay path.

Proof: Without loss of generality, we can let $\sigma_{n,r}^2 = \sigma_{n,d}^2 = 1$. Therefore, the SNRs of the source-to-relay and relay-to-destination channels are defined via the variances of $\mathbf{H}_{SR}$ and $\mathbf{H}_{RD}$. Using (44), we can have

$$\sigma_{R,i}^2\sigma_{rd,i}^2 = \sqrt{\frac{\mu\sigma_{rd,i}^2}{\left(1+\mathbf{B}(i,i)\sigma_{sr,i}^2\right)}+\frac{1}{4}}-\frac{1}{2}. \quad (46)$$

Without $\mathbf{\Upsilon}$ at the source node, we can have $\mathbf{B} = \alpha\mathbf{I}_M$, where $\alpha = P_{S,T}/M$. Assume that the SNR of the relay-to-destination path is much higher than that of the source-to-relay path so that $\mu\sigma_{rd,i}^2 \gg 1+\alpha\sigma_{sr,i}^2$. Then, $\sigma_{R,i}^2\sigma_{rd,i}^2$ can be approximately expressed as

$$\sigma_{R,i}^2\sigma_{rd,i}^2 \approx \sqrt{\frac{\mu\sigma_{rd,i}^2}{1+\alpha\sigma_{sr,i}^2}}. \quad (47)$$

Hence, $\tilde{\mathbf{H}}'$ can be expressed as

$$\begin{aligned}\tilde{\mathbf{H}}'(i,i) &= \left(\sigma_{R,i}^2\sigma_{rd,i}^2+1\right)^{-\frac{1}{2}}\sigma_{R,i}\sigma_{rd,i}\sigma_{sr,i}\\ &= \left(\sqrt{\frac{\mu\sigma_{rd,i}^2}{1+\alpha\sigma_{sr,i}^2}}+1\right)^{-\frac{1}{2}}\left(\sqrt{\frac{\mu\sigma_{rd,i}^2}{1+\alpha\sigma_{sr,i}^2}}\right)^{\frac{1}{2}}\sigma_{sr,i}\\ &= \left(1+\frac{1+\alpha\sigma_{sr,i}^2}{\mu\sigma_{rd,i}^2}\right)^{-\frac{1}{2}}\sigma_{sr,i} \approx \sigma_{sr,i}. \end{aligned} \quad (48)$$

Then, the diagonal entries of $\tilde{\mathbf{H}}'$ have a descending order since $\sigma_{sr,i}$ decreases with i. ■

Proposition 2 shows that the ordering of $\tilde{\mathbf{H}}'(i,i)$ will not be changed, and thus, the new pairing operations are not necessary during the iteration. We now investigate the case of rank deficiency. When at least a subsystem is rank deficient, r becomes smaller than M. From Proposition 2, it is simple to see that the channel angles of the paired subsystems have an ascending order, i.e.,

$$\begin{aligned}\tan^{-1}\left(\frac{\tilde{\mathbf{H}}'(M,M)}{\tilde{\mathbf{H}}'(1,1)}\right) &\le \tan^{-1}\left(\frac{\tilde{\mathbf{H}}'(M-1,M-1)}{\tilde{\mathbf{H}}'(2,2)}\right)\\ &\le \cdots\\ &\le \tan^{-1}\left(\frac{\tilde{\mathbf{H}}'\left(\frac{M}{2}+1,\frac{M}{2}+1\right)}{\tilde{\mathbf{H}}'\left(\frac{M}{2},\frac{M}{2}\right)}\right). \end{aligned} \quad (49)$$

This property indicates that when $r < M$, the corresponding $\mathbf{B}$ will be of the following structure:

$$\mathbf{B} = \mathrm{diag}(\underbrace{2\alpha, 2\alpha, \ldots, 2\alpha}_{M-r}, \underbrace{\alpha, \alpha, \ldots, \alpha}_{2r-M}, \underbrace{0, 0, \ldots, 0}_{M-r}). \quad (50)$$

In the following proposition, we show how to solve $\mathbf{\Sigma}_R$ when $\mathbf{B}$ is of the structure in (50).

Proposition 3: Consider a rank-deficient $\mathbf{F}'_S$ with a rank equal to r, where $(M/2) \le r < M$. Let $\tilde{\mathbf{H}}'_{1:m}$ denote a square matrix consisting of the first m columns and rows of $\tilde{\mathbf{H}}'$. The objective function for the design of $\mathbf{\Sigma}_R$ can be chosen as $\det(\tilde{\mathbf{H}}'^H_{1:M-r}\tilde{\mathbf{H}}'_{1:M-r})\det(\tilde{\mathbf{H}}'^H_{1:r}\tilde{\mathbf{H}}'_{1:r})$ such that the lower bound in (37) can be minimized.

Proof: From (50), it is clear that the rank-deficient subprecoder is used in the first $M-r$ subsystems, whereas the full-rank subprecoder is adopted in the last $r-(M/2)$ subsystems. For the ith subsystem, its free distance can be expressed as

$$d_{\mathrm{free},i}^2 = \begin{cases}\epsilon_{1,i}\tilde{\mathbf{H}}'(i,i)\tilde{\mathbf{H}}'(i,i), & \text{for } 1 \le i \le M-r\\ \epsilon_{2,i}\tilde{\mathbf{H}}'(i,i)\tilde{\mathbf{H}}'(M-i+1,M-i+1), & \text{for } M-r+1 \le i \le \frac{M}{2}\end{cases} \quad (51)$$

(51), shown at the bottom of the previous page, where both $\epsilon_{1,i}$ and $\epsilon_{2,i}$ are constants. Hence, we can rewrite $\prod_{i=1}^{M'} d_{\text{free},i}^2$ as

$$\begin{aligned}\prod_{i=1}^{M'} d_{\text{free},i}^2 &= \prod_{j=1}^{M-r} \tilde{\mathbf{H}}'(j,j)\tilde{\mathbf{H}}'(j,j)\epsilon_{1,j} \times \prod_{l=M-r+1, l\le M'}^{M'} \tilde{\mathbf{H}}'(l,l) \\ &\quad \times \tilde{\mathbf{H}}'(M-l+1, M-l+1)\epsilon_{2,l} \\ &= \underbrace{\prod_{j=1}^{M-r} \epsilon_{1,j} \prod_{k=M-r+1}^{M'} \epsilon_{2,k}}_{\epsilon'} \prod_{l=1}^{M-r} \tilde{\mathbf{H}}'(l,l) \prod_{p=1}^{r} \tilde{\mathbf{H}}'(p,p) \\ &= \epsilon' \sqrt{\det\left(\tilde{\mathbf{H}}_{1:M-r}'^H \tilde{\mathbf{H}}'_{1:M-r}\right) \det\left(\tilde{\mathbf{H}}_{1:r}'^H \tilde{\mathbf{H}}'_{1:r}\right)}. \quad (52)\end{aligned}$$

Similar to (38), it can be verified that ϵ' is a constant. Hence, the objective function is equivalent to maximizing $\det(\tilde{\mathbf{H}}_{1:M-r}'^H \tilde{\mathbf{H}}'_{1:M-r}) \det(\tilde{\mathbf{H}}_{1:r}'^H \tilde{\mathbf{H}}'_{1:r})$ when $(M/2) \le r < M$. ■

When $(M/2) \le r < M$, we can conduct the rank deficiency operations for $M-r$ subsystems, equivalently switching off $M-r$ subchannels at one time. However, this approach may not be efficient. This is because the relay precoder will reallocate its power, and some of the rank-deficient subsystems may become nondeficient in the next iteration. For this reason, we only let one subchannel be switched off at one time. Starting from the first subsystem, if we find that $\tan^{-1}(\tilde{\mathbf{H}}'(M,M)/\tilde{\mathbf{H}}'(1,1))$ is smaller than the angle threshold, then let $r = M-1$ and reformulate $\mathbf{B}$ as

$$\mathbf{B} = \text{diag}\{2\alpha, \alpha, \alpha, \ldots, \alpha, 0\}. \quad (53)$$

Let κ_i be defined as

$$\kappa_i = \begin{cases} 2, & \text{for } i = 1, 2, \ldots, M-r \\ 1, & \text{for } i = M-r+1, M-r+2, \ldots, r. \end{cases} \quad (54)$$

From the results in Proposition 3, the optimization of $\sigma_{R,i}^2$ for $(M/2) \le r < M$ can then be reformulated as

$$\begin{aligned}&\min_{\sigma_{R,i}^2} -\sum_{i=1}^{r} \ln\left(\frac{\kappa_i \sigma_{R,i}^2 \sigma_{rd,i}^2}{\sigma_{R,i}^2 \sigma_{rd,i}^2 \sigma_{n,r}^2 + \sigma_{n,d}^2}\right) \\ &\text{s.t.} \\ &\sum_{i=1}^{r} \sigma_{R,i}^2 \left(\sigma_{n,r}^2 + \mathbf{B}(i,i)\sigma_{sr,i}^2\right) = P_{R,T}. \quad (55)\end{aligned}$$

Then, the solution of the problem in (55) can be expressed as

$$\sigma_{R,i}^2 = \sqrt{\frac{\bar{\mu}_i \sigma_{n,d}^2}{\sigma_{rd,i}^2 \sigma_{n,r}^2 \left(\sigma_{n,r}^2 + \mathbf{B}(i,i)\sigma_{sr,i}^2\right)} + \left(\frac{\sigma_{n,d}^2}{2\sigma_{rd,i}^2 \sigma_{n,r}^2}\right)^2} - \frac{\sigma_{n,d}^2}{2\sigma_{rd,i}^2 \sigma_{n,r}^2} \quad (56)$$

where $\bar{\mu}_i = \mu\kappa_i$. From (53) and (54), we see that $\bar{\mu}_i$ and $\mathbf{B}(i,i)$ are equally affected by κ_i. Hence, we can assume $\bar{\mu}\sigma_{rd,i}^2 \gg 1 + \mathbf{B}(i,i)\sigma_{sr,i}^2$, and then rewrite (47) as

$$\sigma_{R,i}^2 \sigma_{rd,i}^2 \approx \sqrt{\frac{\bar{\mu}_i \sigma_{rd,i}^2}{1 + \mathbf{B}(i,i)\sigma_{sr,i}^2}}.$$

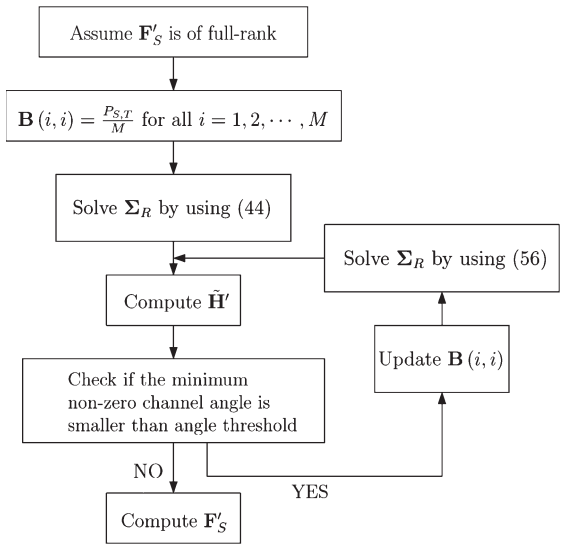

Fig. 3. Algorithm 1: Joint source/relay precoder design without source power allocation $\mathbf{\Upsilon}$.

TABLE II
JOINT SOURCE/RELAY PRECODER DESIGN WITH SOURCE POWER ALLOCATION

Algorithm 2: Joint Source/Relay Precoder Design with $\mathbf{\Upsilon}$.
(1) Set $r = M$, and choose the initial $\mathbf{\Upsilon}^{(0)} = \sqrt{\frac{1}{M'}}\mathbf{I}_M$
(2) Let the initial $\mathbf{B}^{(0)}$ be $\mathbf{B}^{(0)} = \alpha\mathbf{I}_M$;
(3) Set I as the number of iterations;
(3) for $i = 1 : I$
(5) Use Algorithm 1 to obtain $\mathbf{\Sigma}_R^{(i)}$ and $\mathbf{F}_S'^{(i)}$;
(6) Compute $\mathbf{\Upsilon}^{(i)}$ with (18);
(7) Compute $\mathbf{B}^{(i)}$ with $\mathbf{\Upsilon}^{(i)}$ and initial full-rank $\mathbf{F}'_S$
(8) end;

As a result, the statement in Proposition 2 is still valid here. The given procedure is then repeatedly conducted until all nonzero channel angles are larger than the angle threshold or r is equal to $(M/2)$. When $r = M/2$, $\bar{\mu}_i$ becomes a constant for all $i = 1, 2, \ldots, r$. In this case, the structure of $\sigma_{R,i}^2$ in (56) will be reduced to that in (44). Fig. 3 summarizes the complete operations of the proposed algorithm (Algorithm 1).

In previous discussions, we do not conduct source power allocation among all subsystems. This simplification may result in performance loss since the error rate performance can be affected by the subsystem with the minimum free distance. Exploiting $\mathbf{\Upsilon}$ will further complicate the optimization of $\mathbf{\Sigma}_R$ since the behavior of $\mathbf{B}$ is no longer easy to follow. To overcome this, we propose another iterative method to conduct power allocation. We assume that initial $\mathbf{F}'_S$ is of full-rank, and initial $\mathbf{\Upsilon}$, which is denoted by $\mathbf{\Upsilon}^{(0)}$, is a scaled-identity matrix. Hence, initial $\mathbf{B}$, which is denoted by $\mathbf{B}^{(0)}$, is also a scaled-identity matrix. Using Algorithm 1, we can solve $\mathbf{\Sigma}_R^{(1)}$ and then obtain the resultant $\mathbf{F}_S'^{(1)}$. With (18), we can have the updated $\mathbf{\Upsilon}^{(1)}$. Consequently, $\mathbf{B}^{(1)}$ can be obtained and then used in the next iteration. This method is repeatedly conducted until no further improvement can be obtained. The details of the algorithm (Algorithm 2) are summarized in Table II.

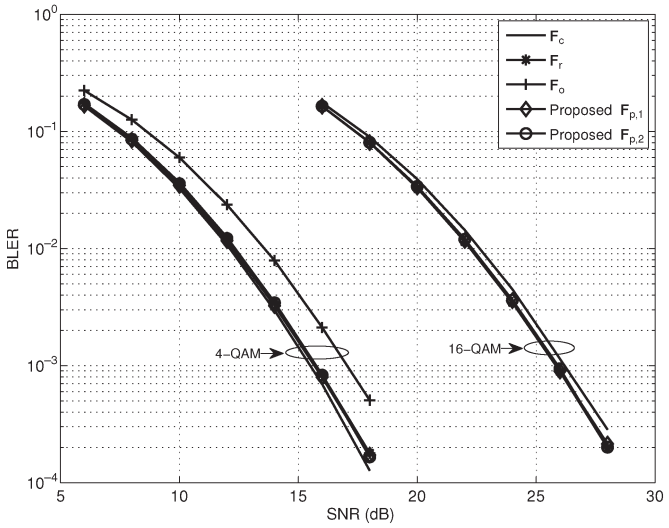

Fig. 4. BLER performance comparisons for MIMO systems with $N_t = 2$, $N_r = 2$, and $M = 2$.

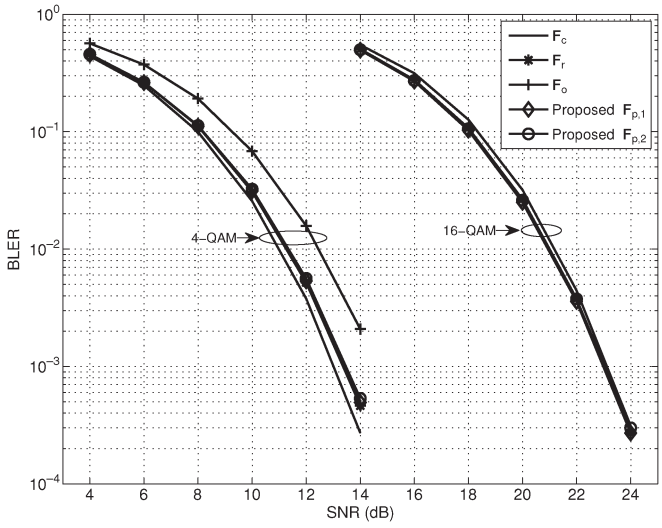

Fig. 5. BLER performance comparisons for MIMO systems with $N_t = 4$, $N_r = 4$, and $M = 4$.

V. Simulation Results

Here, we report simulation results demonstrating the effectiveness of the proposed algorithms. In the simulations, flat-fading MIMO channels are considered, and each entry of $\mathbf{H}$ is assumed to be an i.i.d. complex Gaussian random variable with zero mean and unit variance.

A. Performance Comparisons for MIMO Systems

First, we evaluate the performance of various X-structured precoders. Five subprecoders are compared: 1) complex-valued subprecoder $\mathbf{F}_c$; 2) real-valued subprecoder $\mathbf{F}_r$; 3) orthogonal subprecoder $\mathbf{F}_o$; 4) the proposed subprecoder $\mathbf{F}_{p,1}$; and 5) the proposed subprecoder $\mathbf{F}_{p,2}$. The SNR is defined as SNR $= P_T/\sigma_n^2$. Fig. 4 compares the precoding performance for a MIMO system with $N_t = 2$, $N_r = 2$, and $M = 2$, showing the results of 4- and 16-QAM schemes simultaneously. As we can see, the proposed subprecoders outperform $\mathbf{F}_o$ and give comparable performance with that of $\mathbf{F}_r$. As mentioned, $\mathbf{F}_r$ requires lookup tables in run time. Furthermore, $\mathbf{F}_c$ slightly outperforms other subprecoders in 4-QAM but suffers from performance loss in 16-QAM. It is known that the performance of $\mathbf{F}_o$ for 16-QAM is worse than that of $\mathbf{F}_r$ [19] and is not shown here. Although $\mathbf{F}_{\mathrm{GMD}}$ provides the suboptimum solution, the performance loss of either $\mathbf{F}_{p,1}$ or $\mathbf{F}_{p,2}$ is limited. As discussed, the corresponding free distance for each subprecoder decreases when γ is decreased, and the error rate performance tends to be seriously affected. Instead of using $\mathbf{F}_{\mathrm{GMD}}$, the proposed method uses a rank-deficient subprecoder for a small value of γ, and the performance loss can be mitigated.

Fig. 5 compares the precoding performance for a MIMO system with $N_t = 4$, $N_r = 4$, and $M = 4$. In this scenario, power allocation is conducted with (18). In the figure, we observe similar behaviors as those in Fig. 4. Note that although $\mathbf{F}_c$ can provide optimum performance for 4-QAM, it requires higher detection complexity compared with the other methods. Fig. 6 compares the precoding performance when spatial correlation is considered at the transmitter (and 4-QAM is used). The correlated channel matrix is modeled by $\mathbf{H}_{\mathrm{corr}} = \mathbf{H}\mathbf{R}_t^{(1/2)}$, where $\mathbf{R}_t$ denotes the transmit correlation matrix. In the simulations, two scenarios are considered, i.e., partially decorrelated and highly correlated; the corresponding $\mathbf{R}_t$'s can be found in [34] and [35]. As shown in the figure, our proposed methods still provide comparable performance with $\mathbf{F}_r$.

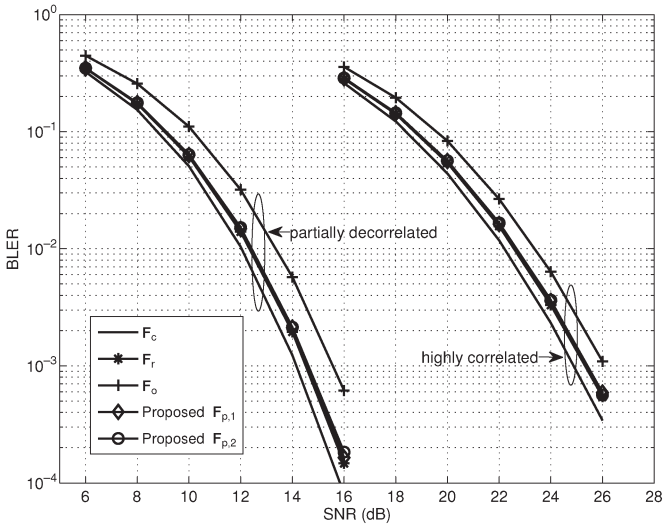

Fig. 6. BLER performance comparisons for correlated MIMO channels with $N_t = 4$, $N_r = 4$, and $M = 4$.

B. Performance Comparisons for MIMO Relay Systems

Next, we evaluate the performance of various precoding methods in a two-hop AF MIMO relay system. Seven systems are considered; the first five systems use ML detection in the receiver, whereas the last two systems use QR-SIC detection. They are as follows: 1) jointly precoded system with $\mathbf{F}_{p,1}$ and $\mathbf{F}_R$ (JP-$\mathbf{F}_{p,1}$-$\mathbf{F}_R$-ML-PA); 2) jointly precoded system with $\mathbf{F}_{p,2}$ and $\mathbf{F}_R$ (JP-$\mathbf{F}_{p,2}$-$\mathbf{F}_R$-ML-PA); 3) jointly precoded system with $\mathbf{F}_{p,2}$ and $\mathbf{F}_R$ without source power allocation (JP-$\mathbf{F}_{p,2}$-$\mathbf{F}_R$-ML-WPA); 4) source precoded system

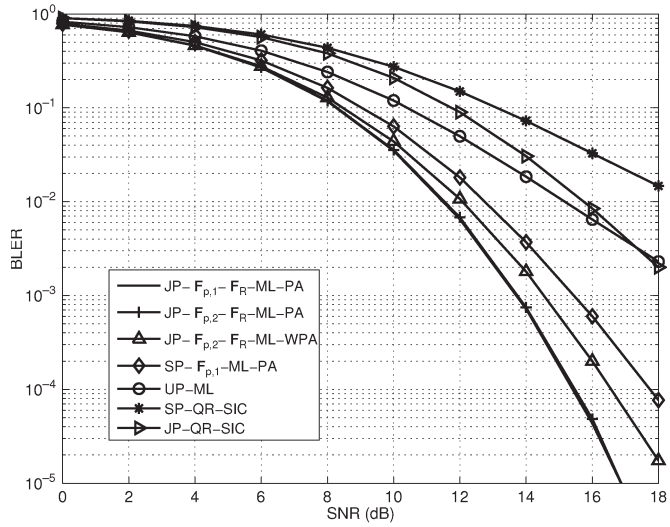

Fig. 7. BLER performance comparisons for MIMO relay systems with 4-QAM.

with $\mathbf{F}_{p,1}$ (SP-$\mathbf{F}_{p,1}$-ML-PA); 5) unprecoded system with ML detection (UP-ML); 6) jointly precoded system (JP-QR-SIC); and 7) source precoded system (SP-QR-SIC). Both the JP-QR-SIC and SP-QR-SIC are obtained from [36] without considering the source-to-destination link. In addition, let SNR_{sr} and SNR_{rd} be defined as $\text{SNR}_{sr} = P_{S,T}/\sigma_{n,r}^2$ and $\text{SNR}_{rd} = P_{R,T}/\sigma_{n,d}^2$, respectively.

Fig. 7 shows the performance comparison for 4-QAM. Here, we let $N_s = 4$, $N_{re} = 4$, $N_d = 4$, $\text{SNR}_{rd} = 25$ dB, and SNR_{sr} be varied. In addition, let $I = 3$ in Algorithm 2 for reasonable precoding complexity. As seen, the proposed JP-$\mathbf{F}_{p,1}$-$\mathbf{F}_R$-ML and JP-$\mathbf{F}_{p,2}$-$\mathbf{F}_R$-ML schemes indeed outperform other precoding methods. It is also observed that about 1-dB performance loss (at the BLER of 10^{-3}) will be induced when source power-allocation matrix $\mathbf{\Upsilon}$ is not included. Compared with the UP-ML scheme, the proposed methods can provide more than 4-dB performance improvement when the BLER is 10^{-3}. Note that the detection complexity of the UP-ML scheme can be much higher than the other methods due to the requirement of 4×4 ML detection. The SP-$\mathbf{F}_{p,1}$-ML-PA scheme suffers from performance loss since only source precoding is considered in the system. As for the JP-QR-SIC and SP-QR-SIC schemes, their performances significantly degrade for a high SNR. Note that in QR-SIC detection, the detection complexity at each receive antenna is $\mathcal{O}(L)$. Moreover, a complete GMD operation is required for finding the source precoder in either the JP-QR-SIC or the SP-QR-SIC scheme. It is clear that the proposed precoding methods are more efficient. We also compare the detection complexity of all methods; the result is shown in Table III. As we can see, the computational complexity of the proposed methods is similar to that of QR-SIC.

Fig. 8 shows the performance comparison for 16-QAM. Here, we let $N_s = 4$, $N_{re} = 4$, $N_d = 4$, $I = 5$, $\text{SNR}_{rd} = 35$ dB, and SNR_{sr} be varied. It can be observed that the proposed methods still provide significant performance improvement. Comparing with the results in Fig. 7, we can see that the performance improvement of the proposed methods is slightly reduced. This result can be explained by the fact that

TABLE III
DETECTION COMPLEXITY COMPARISON IN MIMO RELAY SYSTEMS

Method	Detection Complexity
JP-$\mathbf{F}_{p,1}$-$\mathbf{F}_R$-ML-PA	$\mathcal{O}\left(M'L\sqrt{L}\right)$ for smaller value of L
	$\approx \mathcal{O}\left(M'\sqrt{L}\right)$ for larger value of L
JP-$\mathbf{F}_{p,2}$-$\mathbf{F}_R$-ML-PA	$\mathcal{O}\left(M'\sqrt{L}\right)$
UP-ML	$\mathcal{O}\left(L^M\right)$
JP-QR-SIC	$\mathcal{O}(ML)$
SP-QR-SIC	$\mathcal{O}(ML)$

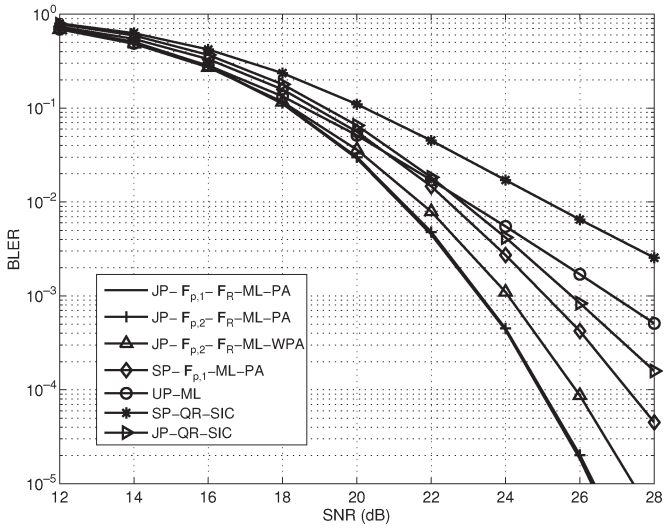

Fig. 8. BLER performance comparisons for MIMO relay systems with 16-QAM.

the free distance yielded by the proposed subprecoders will be rapidly decreased for small values of γ when a large QAM is considered. In other words, the improvement obtained from the rank-deficient subprecoders is reduced.

VI. CONCLUSION

In this paper, we have proposed a systematic method to construct the X-structured precoder for spatial-multiplexing MIMO systems. The proposed subprecoders do not require any numerical search in the design phase and lookup tables in the application phase. In addition, the proposed subprecoders result in almost the same performance and detection complexity as those in the real-valued subprecoder. Except for MIMO systems, we also consider the joint source/relay precoder design in two-hop AF MIMO relay systems. The proposed methods remain the X-structure of the precoder, and the detection complexity is low. This is a great advantage for real-world applications. Simulation results show that the proposed methods can significantly outperform the existing methods. Note that X-structured precoding is suboptimal in the sense that only 2×2 subsystems are considered. To approach the optimum solution more closely, we can consider subsystems whose dimensions are larger than 2×2. In this case, the design of the subprecoder will become very complicated with the conventional methods. It will be much easier to extend the proposed methods in the design of the subprecoder. Research in this subject is now underway.

APPENDIX A
PROOF OF LEMMA 1

Let x be fixed, and define two functions $f(y)$ and $g(y)$ as

$$f(y) = \exp^{-x^{w_1} y^{w_2}} \tag{57}$$
$$g(y) = w_1 \exp^{-x} + w_2 \exp^{-y} \tag{58}$$

where we assume $y \geq x \geq 1$ and $w_1 + w_2 = 1$. The problem now is to prove that $f(y) \leq g(y)$. Assume that both $f(y)$ and $g(y)$ are continuous and differentiable for $y \geq x$. Then, we can rewrite $f(y)$ and $g(y)$ as

$$f(y) = f(x) + \int_x^y f'(t_1)dt_1 \tag{59}$$

$$g(y) = g(x) + \int_x^y g'(t_1)dt_1 \tag{60}$$

where $f'(t_1)$ and $g'(t_1)$ denote the first derivative of $f(t_1)$ and $g(t_1)$, respectively. From (57) and (58), it is easy to verify that $f(x) = g(x)$. Hence, the problem is equivalent to showing that

$$\int_x^y f'(t_1)dt_1 \leq \int_x^y g'(t_1)dt_1. \tag{61}$$

It is simple to see that if $f'(t_1) \leq g'(t_1)$ for $t_1 \geq x$, then (61) holds. Consequently, $f'(t_1)$ and $g'(t_1)$ can be expressed as

$$f'(t_1) = -w_2 x^{w_1} \exp^{-x^{w_1} t_1^{w_2}} t_1^{w_2 - 1} \tag{62}$$
$$g'(t_1) = -w_2 \exp^{-t_1}. \tag{63}$$

Since $-w_2 < 0$, we see that conditions $f'(t_1) \leq g'(t_1)$ and $(-1/w_2)f'(t_1) \geq (-1/w_2)g'(t_1)$ are equivalent. It can be seen that both $(-1/w_2)f'(t_1)$ and $(-1/w_2)g'(t_1)$ are positive values. Define two functions $f_1(t_1)$ and $g_1(t_1)$ as

$$f_1(t_1) \triangleq \ln \frac{-f'(t_1)}{w_2} = w_1 \ln x - w_1 \ln t_1 - x^{w_1} t_1^{w_2} \tag{64}$$
$$g_1(t_1) \triangleq \ln \frac{-g'(t_1)}{w_2} = -t_1. \tag{65}$$

The problem now is equivalent to proving $f_1(t_1) \geq g_1(t_1)$. Using a method similar to that in (59) and (60), we can first rewrite $f_1(t_1)$ and $g_1(t_1)$ as follows:

$$f_1(t_1) = f_1(x) + \int_x^{t_1} f_1'(t_2)dt_2 \tag{66}$$

$$g_1(t_1) = g_1(x) + \int_x^{t_1} g_1'(t_2)dt_2. \tag{67}$$

It can be verified that $f_1(x) = g_1(x)$. Hence, if $f_1'(t_2) \geq g_1'(t_2)$ for $t_2 \geq x$, then $f_1(t_1) \geq g_1(t_1)$. From (64) and (65), we have

$$f_1'(t_2) = -\frac{w_1}{t_2} - x^{w_1} t_2^{w_2 - 1} w_2 \tag{68}$$
$$g_1'(t_2) = -1. \tag{69}$$

For $t_2 = x \geq 1$, we have

$$\begin{aligned} f_1'(t_2)|_{t_2 = x} &= -\frac{w_1}{x} - x^{w_1} x^{w_2 - 1} w_2 \\ &= -\frac{w_1}{x} - w_2 \\ &\geq -(w_1 + w_2) = g_1'(t_2). \end{aligned} \tag{70}$$

For $t_2 > x \geq 1$, we observe that $(x/t_2) < 1$ and that

$$\begin{aligned} f_1'(t_2)|_{t_2 > x} &= -\frac{w_1}{t_2} - x^{w_1} t_2^{w_2 - 1} w_2 \\ &= -\frac{w_1}{t_2} - w_2 \left(\frac{x}{t_2}\right)^{w_1} \\ &\geq -w_1 - w_2 \left(\frac{x}{t_2}\right)^{w_1} \\ &> -w_1 - w_2 = g_1'(t_2). \end{aligned} \tag{71}$$

From (70) and (71), we can see that $f_1'(t_2) \geq g_1'(t_2)$ for any given $t_2 \geq x$. With this result, we can conclude that $f(y) \leq g(y)$ for $y \geq x \geq 1$, which completes the proof of this lemma.

APPENDIX B
PROOF OF LEMMA 2

Using Lemma 1, we can now use mathematical induction to prove Lemma 2. Without loss of generality, we can assume that $d_{\text{free},1} \geq d_{\text{free},2} \geq \cdots \geq d_{\text{free},M'}$. Letting $w_1 = w_2 = 1/2$, $y = d_{\text{free},1}^2/4$, and $x = d_{\text{free},2}^2/4$, we have the following inequality:

$$\exp^{-\sqrt{\frac{d_{\text{free},1}^2}{4}\frac{d_{\text{free},2}^2}{4}}} \leq \frac{1}{2}\exp^{\frac{-d_{\text{free},1}^2}{4}} + \frac{1}{2}\exp^{\frac{-d_{\text{free},2}^2}{4}}. \tag{72}$$

From (72), it is obvious that (37) is true for $M' = 2$. Then, we assume that the statement in Lemma 2 is true for $M' - 1 (M' > 2)$. That is

$$\begin{aligned} &\exp^{-\frac{1}{4}\left(d_{\text{free},1}^2 d_{\text{free},2}^2 \cdots d_{\text{free},M'-1}^2\right)^{\frac{1}{M'-1}}} \leq \frac{1}{M'-1} \\ &\times \left(\exp^{\frac{-d_{\text{free},1}^2}{4}} + \exp^{-\frac{d_{\text{free},2}^2}{4}} + \cdots + \exp^{-\frac{d_{\text{free},M'-1}^2}{4}}\right). \end{aligned} \tag{73}$$

Now, for the MIMO system with M' subsystems, we can have the following equivalence:

$$\begin{aligned} &\exp^{-\frac{1}{4}\left(d_{\text{free},1}^2 d_{\text{free},2}^2 \cdots d_{\text{free},M'}^2\right)^{\frac{1}{M'}}} \\ &= \exp^{-\left(\frac{1}{4}\left(d_{\text{free},1}^2 d_{\text{free},2}^2 \cdots d_{\text{free},M'-1}^2\right)^{\frac{1}{M'-1}}\right)^{\frac{M'-1}{M'}}\left(\frac{1}{4}d_{\text{free},M'}^2\right)^{\frac{1}{M'}}}. \end{aligned} \tag{74}$$

Using Lemma 1 again, we obtain

$$\begin{aligned} &\exp^{-\left(\frac{1}{4}\left(d_{\text{free},1}^2 d_{\text{free},2}^2 \cdots d_{\text{free},M'-1}^2\right)^{\frac{1}{M'-1}}\right)^{\frac{M'-1}{M'}}\left(\frac{1}{4}d_{\text{free},M'}^2\right)^{\frac{1}{M'}}} \\ &\leq \frac{M'-1}{M'}\exp^{-\left(\prod_{i=1}^{M'-1}\frac{d_{\text{free},i}^2}{4}\right)^{\frac{1}{M'-1}}} + \frac{1}{M'}\exp^{\frac{-d_{\text{free},M'}^2}{4}}. \end{aligned} \tag{75}$$

Substituting (73) into (75), we can have the following inequality:

$$\exp^{-\frac{1}{4}\left(d^2_{\mathrm{free},1}d^2_{\mathrm{free},2}\cdots d^2_{\mathrm{free},M'}\right)^{\frac{1}{M'}}} \leq \frac{M'-1}{M'}\frac{1}{M'-1}\sum_{i=1}^{M'-1}\exp^{\frac{-d^2_{\mathrm{free},i}}{4}}+\frac{1}{M'}\exp^{-\frac{d^2_{\mathrm{free},M'}}{4}} \tag{76}$$

$$= \frac{1}{M'}\sum_{i=1}^{M'-1}\exp^{-\frac{d^2_{\mathrm{free},i}}{4}}+\frac{1}{M'}\exp^{-\frac{d^2_{\mathrm{free},M'}}{4}} \tag{77}$$

$$= \frac{1}{M'}\sum_{i=1}^{M'}\exp^{-\frac{d^2_{\mathrm{free},i}}{4}}. \tag{78}$$

It can be verified that the equality in (76) holds when all $d_{\mathrm{free},i}$'s are equal. From (76)–(78), we can have

$$P_w = \sum_{i=1}^{M'}\exp^{-\frac{d^2_{\mathrm{free},i}}{4}} \geq M'\exp^{-\frac{1}{4}\left(\prod_{i=1}^{M'}d^2_{\mathrm{free},i}\right)^{\frac{1}{M'}}} \tag{79}$$

which completes the proof of Lemma 2.

Appendix C
Proof of Property 1

First, using the fact that the arithmetic mean is greater than or equal to the geometric mean, we can prove (39) as follows:

$$P_w = \sum_{i=1}^{M'}\exp^{-\frac{d^2_{\mathrm{free},i}}{4}} \geq M'\left(\prod_{i=1}^{M'}\exp^{-\frac{d^2_{\mathrm{free},i}}{4}}\right)^{\frac{1}{M'}}$$

$$= M'\left(\exp^{-\frac{1}{4}\sum_{i=1}^{M'}d^2_{\mathrm{free},i}}\right)^{\frac{1}{M'}}$$

$$= M'\exp^{-\frac{1}{4}\left(\frac{1}{M'}\sum_{i=1}^{M'}d^2_{\mathrm{free},i}\right)}. \tag{80}$$

Second, using the fact again, we can obtain

$$\left(\prod_{i=1}^{M'}d^2_{\mathrm{free},i}\right)^{\frac{1}{M'}} \leq \frac{1}{M'}\sum_{i=1}^{M'}d^2_{\mathrm{free},i}. \tag{81}$$

From (79)–(81), we then have

$$P_w = \sum_{i=1}^{M'}\exp^{-\frac{d^2_{\mathrm{free},i}}{4}} \geq M'\exp^{-\frac{1}{4}\left(\prod_{i=1}^{M'}d^2_{\mathrm{free},i}\right)^{\frac{1}{M'}}}$$

$$\geq M'\exp^{-\frac{1}{4}\left(\frac{1}{M'}\sum_{i=1}^{M'}d^2_{\mathrm{free},i}\right)}. \tag{82}$$

As seen in (82), the lower bound in (37) is tighter than that in (39).

References

[1] G. J. Foschini, "Layered space–time architecture for wireless communication in a fading environment when using multi-element antennas," *Bell Labs. Tech. J.*, vol. 1, no. 2, pp. 41–59, 1996.

[2] P. W. Wolniansky, G. J. Foschini, G. D. Golden, and R. A. Valenzuela, "V-BLAST: An architecture for realizing very high data rates over the rich-scattering wireless channel," in *Proc. URSI Int. Symp. Signals, Syst., Electron.*, Pisa, Italy, Sep. 1998, pp. 295–300.

[3] L. Zheng and D. N. C. Tse, "Diversity and multiplexing: A fundamental tradeoff in multiple-antenna channels," *IEEE Trans. Inf. Theory*, vol. 49, no. 5, pp. 1073–1096, May 2003.

[4] A. Lozano, A. M. Tulino, and S. Verdu, "Optimum power allocation for parallel Gaussian channels with arbitrary input distributions," *IEEE Trans. Inf. Theory*, vol. 52, no. 7, pp. 3033–3051, Jul. 2006.

[5] F. Perez-Cruz, M. R. D. Rodrigues, and S. Verdu, "MIMO Gaussian channels with arbitrary inputs: Optimal precoding and power allocation," *IEEE Trans. Inf. Theory*, vol. 56, no. 3, pp. 1070–1084, Mar. 2010.

[6] C. Xiao, Y. R. Zheng, and Z. Ding, "Globally optimal linear precoders for finite alphabet signals over complex vector Gaussian channels," *IEEE Trans. Signal Process.*, vol. 59, no. 7, pp. 3301–3314, Jul. 2011.

[7] W. Zeng, C. Xiao, and J. Lu, "A low-complexity design of linear precoding for MIMO channels with finite-alphabet inputs," *IEEE Wireless Commun. Lett.*, vol. 1, no. 1, pp. 38–41, Feb. 2012.

[8] P. Stoica and G. Ganesan, "Maximum-SNR spatial–temporal formatting designs for MIMO channels," *IEEE Trans. Signal Process.*, vol. 50, no. 12, pp. 3036–3042, Dec. 2002.

[9] H. Sampath, P. Stoica, and A. Paulraj, "Generalized linear precoder and decoder design for MIMO channels using the weighted MMSE criterion," *IEEE Trans. Commun.*, vol. 49, no. 12, pp. 2198–2206, Dec. 2001.

[10] A. Scaglione, P. Stoica, S. Barbarossa, G. B. Giannakis, and H. Sampath, "Optimal designs for space–time linear precoders and decoders," *IEEE Trans. Signal Process.*, vol. 50, no. 5, pp. 1051–1064, May 2002.

[11] D. P. Palomar, J. M. Cioffi, and M. A. Lagunas, "Joint Tx–Rx beamforming design for multicarrier MIMO channels: A unified framework for convex optimization," *IEEE Trans. Signal Process.*, vol. 51, no. 9, pp. 2381–2401, Sep. 2003.

[12] D. Wubben, R. Bohnke, J. Rinas, V. Kuhn, and K. D. Kammeyer, "Efficient algorithm for decoding layered space–time codes," *Electron. Lett.*, vol. 37, no. 22, pp. 1348–1350, Oct. 2001.

[13] Y. Jiang, J. Li, and W. W. Hager, "Joint transceiver design for MIMO communications using geometric mean decomposition," *IEEE Trans. Signal Process.*, vol. 53, no. 10, pp. 3791–3803, Oct. 2005.

[14] J.-K. Zhang, A. Kavcic, and K. M. Wong, "Equal-diagonal QR decomposition and its application to precoder design for successive-cancellation detection," *IEEE Trans. Inf. Theory*, vol. 51, no. 1, pp. 154–172, Jan. 2005.

[15] Y. Jiang, J. Li, and W. W. Hager, "Uniform channel decomposition for MIMO communications," *IEEE Trans. Signal Process.*, vol. 53, no. 11, pp. 4283–4294, Nov. 2005.

[16] L. Collin, O. Berder, P. Rostaing, and G. Burel, "Optimal minimum distance-based precoder for MIMO spatial multiplexing systems," *IEEE Trans. Signal Process.*, vol. 52, no. 3, pp. 617–627, Mar. 2004.

[17] B. Vrigneau, J. Letessier, P. Rostaing, L. Collin, and G. Burel, "Extension of the MIMO precoder based on the minimum Euclidean distance: A cross-form matrix," *IEEE J. Sel. Topics Signal Process.*, vol. 2, no. 2, pp. 135–146, Apr. 2008.

[18] S. K. Mohammed, E. Viterbo, Y. Hong, and A. Chockalingam, "MIMO precoding with X- and Y-codes," *IEEE Trans. Inf. Theory*, vol. 57, no. 6, pp. 3542–3566, Jun. 2011.

[19] K. P. Srinath and B. S. Rajan, "A low ML-decoding complexity, full-diversity, full-rate MIMO precoder," *IEEE Trans. Signal Process.*, vol. 59, no. 11, pp. 5485–5498, Nov. 2011.

[20] Q.-T. Ngo, O. Berder, and P. Scalart, "Minimum Euclidean distance based precoders for MIMO systems using rectangular QAM modulations," *IEEE Trans. Signal Process.*, vol. 60, no. 3, pp. 1527–1533, Mar. 2012.

[21] J. N. Laneman, D. N. C. Tse, and G. W. Wornell, "Cooperative diversity in wireless networks: Efficient protocols and outage behavior," *IEEE Trans. Inf. Theory*, vol. 50, no. 12, pp. 3062–3080, Dec. 2004.

[22] B. Wang, J. Zhang, and A. Høst-Madsen, "On the capacity of MIMO relay channels," *IEEE Trans. Inf. Theory*, vol. 51, no. 1, pp. 29–43, Jan. 2005.

[23] X. Tang and Y. Hua, "Optimal design of non-regenerative MIMO wireless relays," *IEEE Trans. Wireless Commun.*, vol. 6, no. 4, pp. 1398–1407, Apr. 2007.

[24] R. Mo and Y. H. Chew, "Precoder design for non-regenerative MIMO relay systems," *IEEE Trans. Wireless Commun.*, vol. 8, no. 10, pp. 5041–5049, Oct. 2009.

[25] W. Guan and H. Luo, "Joint MMSE transceiver design in non-regenerative MIMO relay systems," *IEEE Commun. Lett.*, vol. 12, no. 7, pp. 517–519, Jul. 2008.

[26] F.-S. Tseng, W.-R. Wu, and J.-Y. Wu, "Joint source/relay precoder design in nonregenerative cooperative systems using an MMSE criterion," *IEEE Trans. Wireless Commun.*, vol. 8, no. 10, pp. 4928–4933, Oct. 2009.

[27] R. Mo and Y. H. Chew, "MMSE-based joint source and relay precoding design for amplify-and-forward MIMO relay networks," *IEEE Trans. Wireless Commun.*, vol. 8, no. 9, pp. 4668–4676, Sep. 2009.
[28] F.-S. Tseng and W.-R. Wu, "Linear MMSE transceiver design in amplify-and-forward MIMO relay systems," *IEEE Trans. Veh. Technol.*, vol. 59, no. 2, pp. 754–765, Feb. 2010.
[29] C. Song, K.-J. Lee, and I. Lee, "MMSE based transceiver designs in closed-loop non-regenerative MIMO relaying systems," *IEEE Trans. Wireless Commun.*, vol. 9, no. 7, pp. 2310–2319, Jul. 2010.
[30] C. Xing, S. Ma, and Y.-C. Wu, "Robust joint design of linear relay precoder and destination equalizer for dual-hop amplify-and-forward MIMO relay systems," *IEEE Trans. Signal Process.*, vol. 58, no. 4, pp. 2273–2283, Apr. 2010.
[31] Y. Rong, "Robust design for linear non-regenerative MIMO relays with imperfect channel state information," *IEEE Trans. Signal Process.*, vol. 59, no. 5, pp. 2455–2460, May 2011.
[32] S. Boyd and L. Vandenberghe, *Convex Optimization*. Cambridge, U.K.: Cambridge Univ. Press, 2004.
[33] N. Al-Dhahir and J. M. Cioffi, "Optimum finite-length equalization for multicarrier transceivers," *IEEE Trans. Commun.*, vol. 44, no. 1, pp. 56–64, Jan. 1996.
[34] J. P. Kermoal, L. Schumacher, K. I. Pedersen, P. E. Mogensen, and F. Frederiksen, "A stochastic MIMO radio channel model with experimental validation," *IEEE J. Sel. Areas Commun.*, vol. 20, no. 6, pp. 1211–1226, Aug. 2002.
[35] H. Lee and E. J. Powers, "Low-complexity mutual information-based antenna grouping scheme for a D-STTD system," in *Proc. IEEE Global Telecommun. Conf.*, San Francisco, CA, USA, Nov. 2006, pp. 1–5.
[36] F.-S. Tseng and W.-R. Wu, "Nonlinear transceiver designs in MIMO amplify-and-forward relay systems," *IEEE Trans. Veh. Technol.*, vol. 60, no. 2, pp. 528–538, Feb. 2011.

Chun-Tao Lin (M'12) received the B.S. degree in electrical engineering from National Chung Cheng University, Chiayi, Taiwan, in 2002 and the M.S. and Ph.D. degrees in communications engineering from National Chiao Tung University, Hsinchu, Taiwan, in 2004 and 2012, respectively.

He is currently a Postdoctoral Research Fellow with the Institute of Communications Engineering, National Chiao Tung University. His research interests include broadband communications and multiple-input–multiple-output signal processing.

Wen-Rong Wu (M'89) received the B.S. degree in mechanical engineering from Tatung Institute of Technology, Taipei, Taiwan, in 1980 and the M.S. degrees in mechanical and electrical engineering and the Ph.D. degree in electrical engineering from The State University of New York at Buffalo, Buffalo, NY, USA, in 1985, 1986, and 1989, respectively.

Since August 1989, he has been a faculty member with the Institute of Communications Engineering, National Chiao Tung University, Hsinchu, Taiwan. His research interests include statistical signal processing and digital communications.